1. INTRODUCTION

Bituminous paving mixtures are used as surface layers or base layers in pavement structures to distribute stresses induced by loading and to protect underlying unbound layers from the effects of water. To adequately perform both of these functions over the pavement design life, the mixture must also withstand the effects of air and water while resisting the permanent deformation and cracking that tend to be caused by loading and the environment.

Many factors affect the ability of a bituminous paving mixture to meet these structural requirements. Mixture design, construction practices, properties of the component materials, and the use of additives all play important roles in the ultimate structural characteristics of a pavement. The interaction between mixture design and pavement design also needs to be recognized as a factor in deriving the most cost-effective solutions.

Although great strides have been made in understanding the behavior of bituminous mixtures and the factors that affect their performance, much work still remains to be done.

To perform satisfactorily in pavement systems, bituminous mixtures should exhibit the following characteristics:

1) Ability to distribute stresses;
2) Stability in resisting permanent deformation;
3) Resistance to cracking; and
4) Resistance to freeze-thaw cycles and moisture damage.

Numerous factors (binder characteristics, aggregate characteristics, additives, temperature, moisture, loading history, aging characteristics, stress state, and compaction method) and associated properties affect a bituminous mixture's ability to meet these structural requirements. These relate to the fields of materials, environment, loading, and construction.

Based on the analysis, the influences considered in this report can be divided into the following main areas:

1) Moisture susceptibility of asphalt mixtures
2) Effect of various factors on asphalt mixture performance
3) Durability of asphalt mixtures
4) Evaluation indicators for asphalt mixture performance at low and high temperatures

2. MOISTURE SUSCEPTIBILITY OF ASPHALT MIXTURES

2.1 Introduction

One major cause of asphalt pavement failure is damage to the asphalt mixture by water. Such moisture damage occurs in two ways: softening and stripping. The former is characterized by a loss of cohesion, which reduces the strength and stiffness of the asphalt mixture, whereas the latter involves a loss of adhesion and physical separation of asphalt and aggregate[1]. The latter has a greater influence on pavement performance through a process in which asphalt adhesion deteriorates, the asphalt film separates from the aggregate surface, and finally raveling of the asphalt mixture occurs, generally leading to the appearance of potholes.

This moisture susceptibility of asphalt mixtures is related to aggregate properties, asphalt properties, asphalt film thickness, interactions between asphalt and aggregate, air voids in the asphalt mixture, and traffic levels[2]. Among these, interaction between asphalt and aggregate is the main factor influencing the stripping of asphalt mixtures, so it is particularly important to analyze this phenomenon.

Aggregates and asphalt in mixtures susceptible to stripping can be treated with a variety of anti-stripping additives. These additives commonly include the following types:

1) Liquid anti-stripping additives
2) Portland cement
3) Hydrated lime

While hydrated lime is considered an effective way to minimize moisture damage, many liquid anti-stripping additives are also recognized as suitable, and in many cases they appear to be equal to or better than hydrated lime. It has recently been reported that the indirect tensile strength and tensile strength ratio of mixtures containing liquid anti-stripping additives are not significantly different from those of mixtures containing aggregates fully coated with hydrated lime, and mixtures made with hydrated lime show no particular superiority over those using liquid anti-stripping according to tensile strength ratio (TSR) values measured in several overlay sections containing various anti-stripping additives. Further, liquid anti-stripping additives can be used as a substitute for hydrated lime without sacrificing moisture resistance[3]. Thus, the effect of anti-stripping additives needs to be examined in detail.

In this study, we examined the fundamental properties of asphalt-aggregate interactions, including moisture adsorption and moisture damage, by various test methods. The influence of asphalt acidity on the moisture susceptibility of the asphalt mixture was investigated. The effectiveness of hydrated lime and other selected anti-stripping additives was measured through various tests. From the results, suitable methods of clarifying the moisture susceptibility of asphalt mixtures were developed.

2.2 Materials

(1) Asphalt

Five types of asphalt from different crude oils, denoted KL, LH, MM, SJ, and SL, were used in this

study of moisture susceptibility. Their properties, including both physical and chemical values, are given in **Table 1**. The chemical property of acidity was measured according to reference[4]; acidity was found to rank as KL>SJ>LH>SL>MM.

The asphalt KL was also used in the study of anti-stripping additives.

(2) Aggregates

Three kinds of aggregates were used in the asphalt mixtures: limestone, granite, and schist. The chemical properties of these materials can be characterized as basic, acidic, and neutral, respectively. Granite is known to produce water-susceptible asphalt mixtures, whereas limestone has good stripping resistance in asphalt mixtures.

The center value of specified grading and the physical properties of these aggregates are shown in **Figure 1** and **Table 2**, respectively.

(3) Additives

Four different anti-stripping additives were evaluated: Portland cement, hydrated lime, and two liquid anti-stripping additives.

The Portland cement and hydrated lime were added to the aggregate at a ratio of 1% by mass. Two commercially available liquid anti-stripping additives, denoted AST-3 and PA-1, were used, and their chemical structures are shown in **Figure 2**. They were added at a ratio of 0.3% of asphalt by mass.

Two methods were used to introduce lime into the asphalt mixtures, as specified below.

1) Dry lime was added to the cold aggregate and mixed well to coat the aggregate, and then both were heated before mixing with the asphalt.
2) Lime, combined with water at a ratio of 7 to 3, was mixed with the cold aggregate and both were dried at 130°C for at least 15 hours before mixing with the asphalt.

Portland cement was introduced by the dry lime treatment method.

Liquid anti-stripping additives were added to the asphalt after preheating to about 140°C and they were continuously stirred to ensure homogeneity before mixing with the aggregate.

Table 3 summarizes the anti-stripping additives used. The identifications given in the table are used in the following figures.

(4) Asphalt mixtures

The asphalt mixtures were designed in accordance with the standard Marshall method specified for road pavements: 75 blows on each side of the specimen in preparation and a Marshall stability of 7.5 kN. The optimum asphalt content was determined to be 5.0% for asphalt mixtures used to study moisture susceptibility and 4.8% for those used to study the effects of anti-stripping additives. In the latter case, the asphalt content was not adjusted for the presence or absence of additives.

Table 1 Properties of asphalts

a) Original

Item	KL	LH	MM	SJ	SL
Density (15°C, g/cm^3)	0.9815	1.005	1.013	0.9978	1.001
Solution (%)	99.10	99.53	99.91	99.08	99.78
Wax content (%)	1.28	3.85	4.08	4.19	5.55
Flash point (°C)	300	280	350	320	296
Fraass breaking point (°C)	-15	-19.8	-13	-14.8	-16.7
Softening point (°C)	49.5	46	50	50.5	49
Penetration (25°C, 1/10 mm)	89	138	81	97	96
PI	0.19	-1.43	-0.8	-1.07	-1.69
Ductility (15°C, cm)	>150	>150	>100	58	22
Viscosity (60°C, Pa·s)	309.9	65	129.1	62.4	59.3
Acidity (m*l*·mol/L/g)	2.510	1.256	0.273	1.789	0.564

b) After thin-film oven test (TFOT)

Item	KL	LH	MM	SJ	SL
Weight loss (%)	-0.05	-0.20	0.15	-0.06	0.10
Softening point (°C)	51.5	48.5	52	53	52
Penetration ratio (%)	75.2	60.9	66.7	60.8	64.6
Ductility (15°C, cm)	>100	43.6	29.8	12.8	6.8.

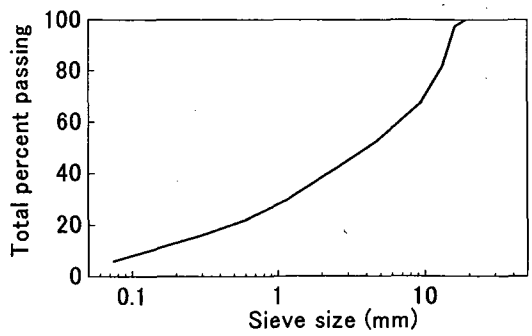

Figure 1 Central value of specified aggregate grading

Table 2 Physical properties of aggregates

Aggregate	Specific gravity (g/cm^3)	Absorption (%)	SiO_2 content (%)
Granite	2.751	0.43	76.5
Schist	2.834	0.49	63.1
Limestone	2.712	0.51	6.5
Filler	2.745	—	—

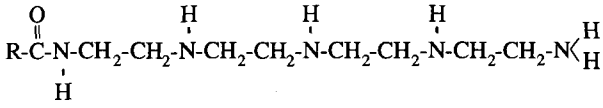

a) AST-3

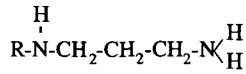

b) PA-1

Figure 2 Chemical structures of additives

Table 3 Anti-stripping additives

ID	Additive	Amount
A	Portland cement	1% of aggregate
B	Hydrated lime	1% of aggregate
C	Lime slurry	1% of aggregate
D	AST-3	0.3% of asphalt
E	PA-1	0.3% of asphalt
F	None	-

2.3 Test Methods

A variety of tests were performed, including a water immersion test, an electro-optic colorimetry test, a net adsorption test, a retained Marshall stability test, a Lottman test, and an immersed wheel tracking test.

2.4 Water Susceptibility of Asphalt Mixtures

In this section, a number of tests are used to reveal the characteristics of asphalt-aggregate interactions and the influence of asphalt acidity on the moisture susceptibility of asphalt mixtures.

(1) Stripping resistance of the asphalt-aggregate bond

A water immersion test was carried out, and the results are given in **Table 4**. The stripping ratio depends on both the type of aggregate and the type of asphalt. Whereas limestone showed good resistance to stripping, asphalt mixtures containing granite were very susceptible to stripping. In terms of stripping resistance, the asphalt mixtures are ranked as KL>SJ>LH>MM>SL.

An electro-optic colorimetry test was carried out, and the results are given in **Table 5**. The type of aggregate and the type of asphalt affect the moisture susceptibility of the asphalt mixture in a way similar to that seen in the water immersion test.

A net adsorption test was also carried out, and the results are given in **Table 6**; here also a similar trend is seen. The chemical properties of the aggregate play a significant role in determining the strength of the asphalt-aggregate bond; the stripping ratio ranges from 8.0 to 31.3% with limestone, from 19.7 to 62.0% with schist, and from 58.9 to 100% with granite.

Table 4 Stripping ratio in water immersion test

Aggregate	KL	LH	MM	SJ	SL
Granite	50	65	55	60	70
Limestone	5	5	15	5	15
Schist	15	20	35	20	70

(unit: %)

Table 5 Stripping ratio in electro-optic colorimetry test

Aggregate	KL	LH	MM	SL	SJ
Granite	35.6	85.3	57.4	96.7	54.9
Limestone	22.2	72.6	39.2	64.7	43.1
Schist	48.7	64.3	42.9	84.4	34.6

(unit: %)

Table 6 Stripping ratio in net adsorption test

Asphalt	Granite			Limestone			Schist		
	Initial adsorption	Net adsorption	Stripping ratio	Initial adsorption	Net adsorption	Stripping ratio	Initial adsorption	Net adsorption	Stripping ratio
KL	0.0618	0.0153	75.2	0.0834	0.0770	8.0	0.2252	0.1182	19.7
LH	0.0318	0.0127	60.1	0.8055	0.0697	15.5	0.1949	0.1223	37.9
MM	0.0469	0.0094	79.9	0.1080	0.0685	30.3	0.1391	0.0529	62.0
SJ	0.1196	0.0490	58.9	0.1057	0.0799	17.0	0.1732	0.1366	21.2
SL	0.0097	0.0	100.0	0.1565	0.1069	31.1	0.1432	0.0606	57.7

(unit: original adsorption = mg/g, net adsorption = mg/g, stripping ratio = %)

Table 7 Classification of moisture susceptibility[5)]

Stripping ratio (%)	Asphalt-aggregate adhesion
<30	Good
45-30	Marginal
>45	Poor

According to the classifications of asphalt-aggregate adhesion by moisture susceptibility set by SHRP, as shown in **Table 7**, limestone has superior stripping resistance, while schist is also evaluated as having marginally higher stripping resistance than granite.

The type of asphalt also has a large influence on moisture susceptibility. Whereas KL, LH, and SJ asphalts appear to have higher stripping resistance, MM and SL asphalts exhibit lower values.

The stripping ratios measured in these three tests are plotted against asphalt acidity, representing the chemical properties of the asphalt, in **Figures 3, 4,** and **5**. These figures show that the stripping ratios decrease as acidity increases. It should be noted that the water immersion test involves visual observations, so the results may include significant errors. Further, the electro-optic colorimetry test suffers from disadvantages — such as the fact that the results reflect only the separation ratio of asphalt film from the aggregate surface, not the actual stripping ratio of asphalt from aggregate. In contrast, in the net adsorption test, asphalt adsorption from the aggregate surface is obtained directly by measuring changes in the concentration of the asphalt solution, so error is minimized. Thus, this method is a suitable method of evaluating the moisture susceptibility of the asphalt-aggregate bond.

(2) Mechanical properties of asphalt mixtures

The results of the retained Marshall stability test are given in **Table 8**. Of the aggregates, limestone provides superior moisture stability, whereas granite gives the lowest moisture stability. The moisture stability of the asphalt mixture containing limestone ranks as KL>LH>SL>SJ>MM with aggregate type, and the stability of mixtures with other aggregates is similar.

The results of the Lottman test are shown in **Table 9**. The influence of aggregate type on moisture susceptibility is the same as that in the retained Marshall stability test. According to the specifications set by SHRP, the asphalt mixture with limestone, which has a TSR of 70% or more, meets the requirements except with asphalt MM. In contrast, mixtures containing the other aggregates do not meet the specifications. Asphalt mixtures containing asphalt KL have the best moisture stability, whereas those with asphalts MM and SL have the poorest.

The relationship between asphalt acidity and the moisture susceptibility of the asphalt mixture is shown in **Figures 6** and **7**.

Figure 6 shows that the retained Marshall stability increases with asphalt acidity and depends on the type of aggregate. This trend is similar to that for asphalt-aggregate bonding. Since the retained Marshall stability of asphalt mixtures with limestone scarcely changes with asphalt acidity, the retained Marshall stability test is unable to accurately distinguish moisture susceptibility.

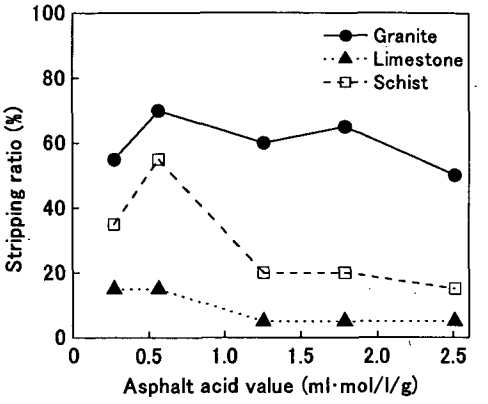

Figure 3 Acidity and stripping ratio in water immersion test

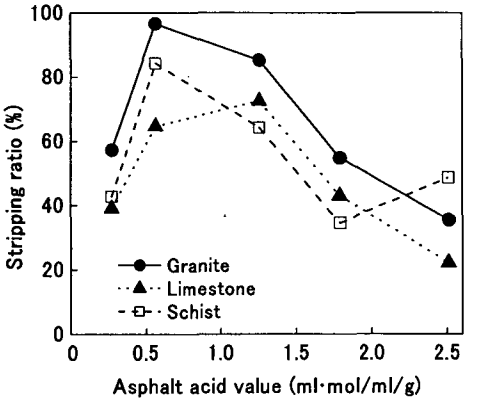

Figure 4 Acidity and stripping ratio in electro-optic colorimetry test

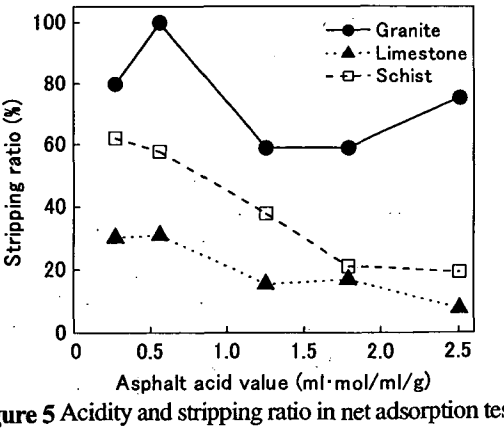

Figure 5 Acidity and stripping ratio in net adsorption test

Table 8 Retained Marshall stability

Asphalt	Granite			Limestone			Schist		
	S_1	S_2	S_0	S_1	S_2	S_0	S_1	S_2	S_0
KL	10.63	6.42	63.5	8.27	7.87	90.3	10.61	7.88	74.3
LH	10.12	4.40	43.4	7.99	7.41	89.4	11.74	6.42	54.7
MM	10.70	0	0	10.63	8.01	79.9	11.95	2.94	24.6
SJ	10.11	6.46	63.9	8.96	7.28	81.3	10.96	8.03	73.3
SL	10.39	2.16	20.8	8.83	7.82	88.5	11.98	5.28	44.1

(unit: S_1, S_2-kN, S_0-%)

Table 9 Tensile strength ratio in Lottman test

Asphalt	Granite			Limestone			Schist		
	R_1	R_2	TSR	R_1	R_2	TSR	R_1	R_2	TSR
KL	0.564	0.217	38.5	0.465	0.450	96.8	0.482	0.353	73.2
LH	0.515	0.158	30.7	0.516	0.394	75.4	0.527	0.250	47.4
MM	0.621	0.077	12.1	0.671	0.385	57.4	0.637	0.092	14.8
SJ	0.624	0.210	33.7	0.483	0.429	88.8	0.638	0.364	57.1
SL	0.576	0.037	6.4	0.459	0.351	76.5	0.616	0.173	28.1

(unit: R_1, R_2-MPa, TSR-%)

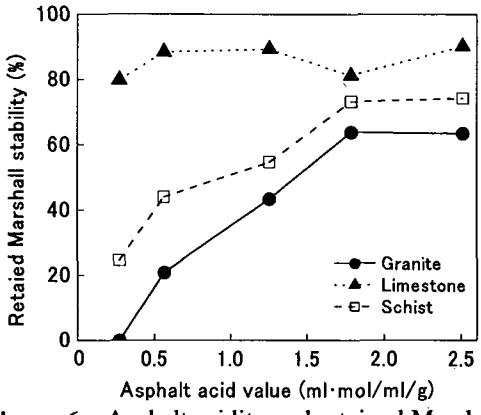

Figure 6 Asphalt acidity and retained Marshall stability

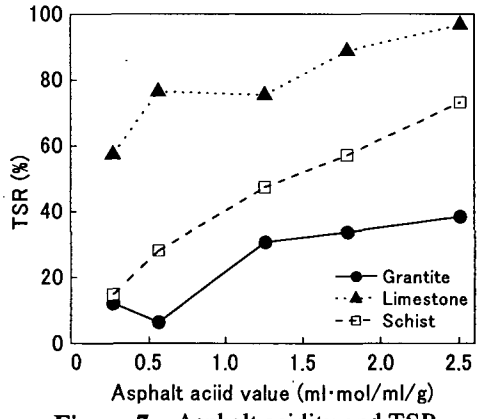

Figure 7 Asphalt acidity and TSR

In **Figure 7**, the TSR of the asphalt mixture containing limestone increases with asphalt acidity. Thus, the Lottman test is suitable for evaluating the moisture susceptibility of asphalt mixtures.

2.5 Effect of Additives on Moisture Susceptibility

This section clarifies the effects of anti-stripping additives on moisture susceptibility through a series of laboratory tests. The applicability of the additives to actual construction is also verified using two aging methods.

(1) Property changes with water immersion

As shown in **Figure 8**, the Lottman test shows that all the anti-stripping additives improve the moisture susceptibility of the asphalt mixtures, while the degree of improvement depends on both the additive and the aggregate.

Lime slurry (C) gives mixtures the best resistance to moisture damage, and hydrated lime (B) and liquid anti-stripping additive AST-3 (D) also offer good moisture stability. However, Portland cement (A) only slightly improves moisture susceptibly. Further, the aggregate strongly influences moisture stability once an additive has been added; that is, the TSR of the asphalt mixture containing granite never exceeds that of mixtures containing other aggregates.

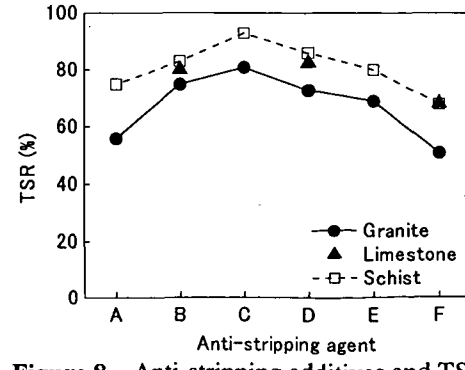

Figure 8 Anti-stripping additives and TSR

Figure 9 shows the retained Marshall stability for the mixtures. This demonstrates that all anti-stripping additives aside from Portland cement (A) provide similar improvements to the moisture susceptibility. Thus, the retained Marshall stability test yields almost the same results even when the treatment method changes.

Figures 10 and **11** show the results of immersed wheel tracking tests on granite and schist aggregates, respectively. These figures show that rut depth increases with the number of tracking cycles irrespective of aggregate type, and that asphalt mixtures containing schist offer better rutting and water resistance than those containing granite.

Figure 12 shows the ultimate rut depth at the end of the test. Asphalt mixtures containing schist have shallower ruts than those containing granite, despite the larger number of tracking cycles. Lime, regardless of whether dry or slurry (B and C), provides a remarkable improvement in moisture stability. On the contrary, Portland cement (A) and liquid anti-stripping additives (D and E) have less effect.

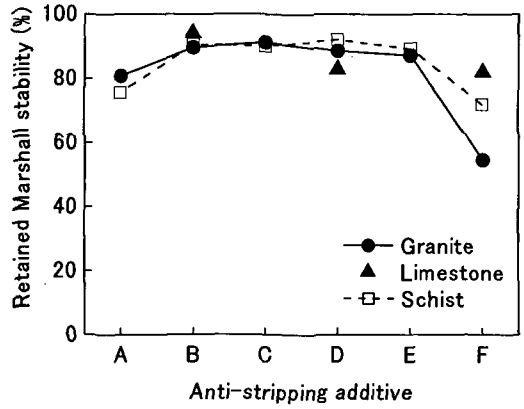

Figure 9 Anti-stripping additives and retained Marshall stability

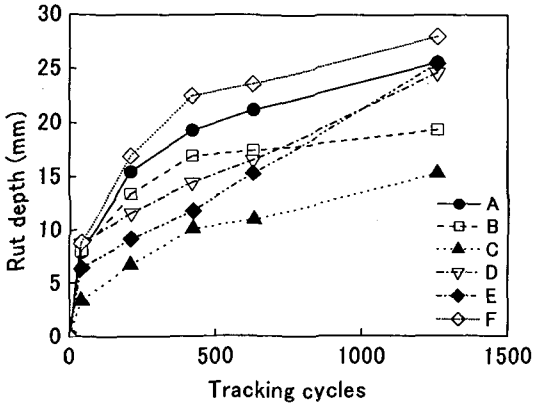

Figure 10 Rut depth with tracking cycles (Granite)

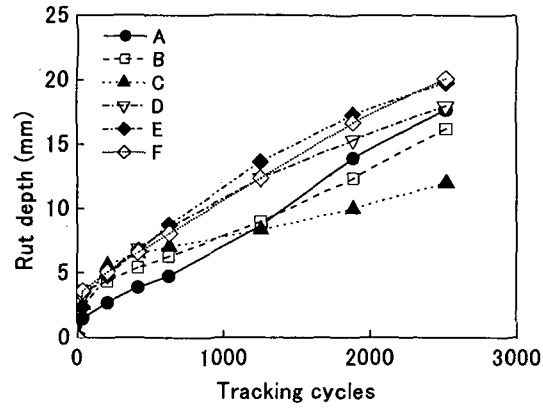

Figure 11 Rut depth with tracking cycles (Schist)

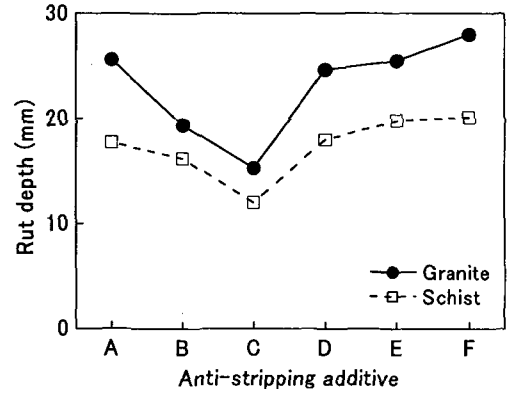

Figure 12 Anti-stripping additives and rut depth

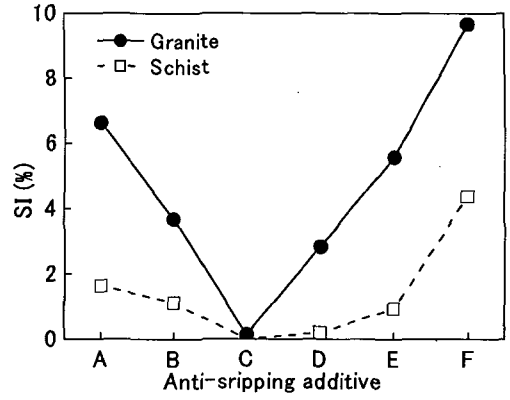

Figure 13 Anti-stripping additives and SI

The stripping index, SI, indicates that lime slurry (C) can significantly improve the moisture susceptibility of asphalt mixtures, as shown in **Figure 13**. Portland cement (A) has little effect, as in the case of rut depth. Thus, the immersed wheel tracking test indicates the same influence of aggregate type on moisture susceptibility as the Lottman test.

(2) *Influence of aging method on moisture susceptibility*

Figure 14 shows the retained Marshall stability test results for various limestone asphalt mixtures with age.

In general, retained Marshall stability decreases after short-term aging, and falls further with prolonged aging. Though differences in retained Marshall stability are clear before aging, any difference becomes imperceptible in the long term.

Figure 15 shows TSR as measured in the Lottman test for limestone asphalt mixtures. TSR values increase after short-term aging irrespective of treatment type, due to stiffening of the asphalt concrete as it ages, but they decrease in the long term. It is also found that lime (B) remains more effective than a liquid anti-stripping additive (D) even after long-term aging. These results indicate that the Lottman test is a more useful means of evaluating moisture susceptibility than the retained Marshall stability test.

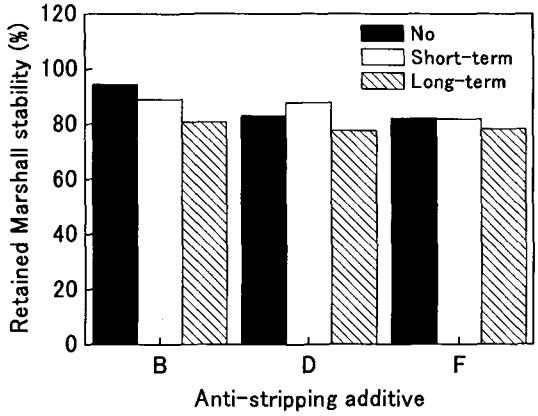

Figure 14 Influence of age on retained Marshall stability

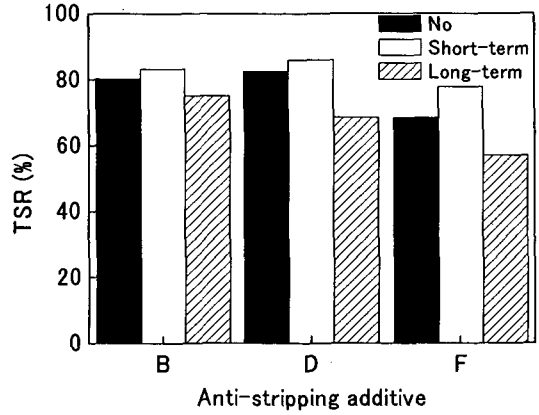

Figure 15 Influence of age on TSR

2.6 Summary

A series of laboratory tests was conducted to evaluate the moisture susceptibility of asphalt mixtures and the effectiveness of anti-stripping additives. The following major conclusions can be drawn from the results:

1) Both asphalt type and aggregate type have a dominant influence on asphalt-aggregate bonding and the moisture susceptibility of asphalt mixtures.
2) Asphalt acidity can be used to evaluate the moisture susceptibility of asphalt mixtures; moisture susceptibility improves with asphalt acidity.
3) Limestone aggregate offers superior stripping resistance, while schist has marginally higher stripping resistance than granite.
4) The net adsorption test is superior to the water immersion test and the electro-optic colorimetry test as a means of evaluating asphalt-aggregate bonding.
5) Hydrated lime slurry added to an asphalt mixture is a more effective method of decreasing moisture susceptibility than liquid anti-stripping additives and Portland cement.
6) The Lottman test and immersed wheel tracking test are better than the retained Marshall stability test as methods of evaluating the moisture susceptibility of asphalt mixtures.
7) The moisture susceptibility of asphalt mixtures containing additives decreases over the long term. Thus, age might be a useful means of evaluating the in-situ moisture susceptibility of asphalt mixtures.

3. EFFECTS OF VARIOUS FACTORS ON ASPHALT CONCRETE PERFORMANCE

3.1 Introduction

As aircraft become larger and operational frequencies increase, the loading on airport pavements, that is, increases in both wheel loads and tire pressures, is beginning to exceed the values assumed in traditional pavement design. As a result, rutting, deformation, and fatigue cracking are becoming more prevalent. It is therefore well known that the asphalt concretes currently used for airport pavements have insufficient durability to withstand heavy duty loading, and this is affected by several factors such as the properties of the aggregates and asphalt, the asphalt content, and environmental conditions[6].

Given this situation, pavement engineers are looking for new approaches by which to address the problems. In the past few years, various modifications to asphalt concrete have been proposed with the aim of alleviating the problems[7]. However, no modified asphalt has been standardized in the specifications for airport paving work, so this study examines the mechanical properties of asphalt concretes made with modified asphalts.

Unfortunately, the simple introduction of a modified binder alone will not solve the most serious problems facing paving engineers: rutting and cracking. Recognizing this, the strategic highway research

program (SHRP) introduced a new mix design system with binder specifications for performance grading as well as a series of advanced tests for application to asphalt concretes. The system focuses on binder properties, and the quality and gradation of aggregates, and the specifications characterize the binder in relation to rutting and cracking[8]. Aggregate quality and grading are particularly important with regard to rutting. In particular, aggregate grading is the most important factor in asphalt concrete design because it affects almost all of the ultimate physical properties. Therefore, asphalt concretes with various aggregate gradings, such as stone mastic asphalt concrete (SMA), stone asphalt concrete (SA), and Superpave asphalt concrete (SP), are studied in comparison with dense graded asphalt concrete (DGA); that is, their resistance to rutting, moisture damage, low temperature cracking and abrasion, and water permeability are evaluated.

The resistance of asphalt pavements to rutting is improved if the asphalt concrete layers are compacted well during construction; this is important because aircraft tire pressures are higher than those of motor vehicles. Therefore, the influence of compaction effort on the mechanical properties of asphalt concretes is also examined.

3.2 Materials and Mixture Design

(1) Materials

A straight 60/80 asphalt and modified asphalt II were used in the study, the properties of which are given in **Table 10**. The properties of the aggregates used in the laboratory tests are given in **Table 11**. The aggregate gradings included in the asphalt concretes used here are presented in **Table 12**.

Asphalt concrete SMA was prepared using fibers as a stabilizer at 0.4% by total weight of the asphalt concrete. In the Superpave asphalt concretes, two kinds of aggregate gradings were used: SP-A and SP-B, respectively designating gradings passing below and above the restricted zone.

Table 10 Properties of binders

Property		Straight	Modified
Penetration (1/10mm, 25°C)		73	64
Softening point (°C)		47	64
Ductility (cm, 15°C)		140+	92
Solution (%)		99.8	-
Thin film oven test (163°C, 5h)	Loss (%)	0.02	0.01
	Penetration ratio (%)	64.4	82.7
Density (g/cm^3)		1.034	1.028

Table 11 Properties of aggregates

Item	Coarse aggregate				Fine aggregate			Filler
	#4	#5	#6	#7	Screening	Coarse sand	Fine sand	
Apparent specific gravity (g/cm^3)	2.709	2.723	2.716	2.713	2.740	2.626	2.639	2.710
Absorption (%)	0.61	0.57	0.65	1.24	1.76	1.17	1.58	-
Abrasion (%)	16.3	11.7	13.2	14.8	-	-	-	-
Soundness (%)	8.4	6.3	5.6	3.7	2.1	2.9	3.9	-

Table 12 Aggregate gradings of the asphalt concretes

Sieve size (mm)	DGA	SMA	SA	SP-A	SP-B
37.5	-	-	-	-	-
26.5	100	100	100	100	100
19	97.5	97.5	97.5	95	95
16	-	-	86	-	-
13.2	82.5	82.5	74.5	-	-
9.5	-	-	58.5	-	-
4.75	55	35	35	-	-
2.36	42.5	27.5	26.5	33	38
1.18	-	-	20	20	30
0.6	24	-	16	15	22
0.3	15.5	16.5	13.5	11	15
0.15	11	-	11.5	-	-
0.075	6	10.5	8	4	5

Table 13 Results of Marshall test

	DGA	SMA	SA	SP-A	SP-B
Optimum asphalt content (%)	5.4	5.3	5.2	5.3	5.3
Density (g/cm^3)	2.407	2.397	2.428	2.417	2.422
Maximum density (g/cm^3)	2.481	2.487	2.501	2.492	2.495
Air void (%)	3.0	3.6	2.9	3.0	2.9
VMA (%)	15.6	15.9	15.1	15.4	15.3
Stability (kN)	11.76	9.03	9.64	10.63	13.21
Flow (1/10mm)	31	36	37	32	33
VFA (%)	80.8	77.4	80.8	80.5	81.0
Retained stability (%)	86.0	88.0	85.4	89.4	88.0

(2) Mix design

Marshall mix design was applied to the asphalt concretes so as to determine the optimum asphalt content. **Table 13** summarizes the properties of the asphalt mixtures at the optimum asphalt content. This table shows that asphalts DGA and SP-B have greater stability and lower flow than the asphalts SMA, SA, and SP-A, but there is no significant difference in retained stability among them. SMA has low VFA, which is related to the larger air void content and lower asphalt content.

3.3 Test Methods

The mechanical properties of the different asphalt concretes were evaluated through rutting tests (standard tire pressure of 0.63 MPa and high pressure of 1.38 MPa), moisture susceptibility tests, low-temperature bending tests, water permeability tests, and abrasion tests.

3.4 Effect of Modified Asphalt

The effects of modified asphalt on the properties of asphalt concretes were studied by using DGA. The results are summarized in **Table 14**. Asphalt concrete made with modified asphalt has a much higher dynamic stability than conventional asphalt, and also better resistance to water damage. Further, modified asphalt concrete exhibits higher stress and strain and lower stiffness at low temperatures. The test results also indicate that the binder is the main contributor to the performance of asphalt concrete, because the modified asphalt increases the resistance of asphalt concrete to both rutting at high temperatures and cracking at low temperatures.

3.5 Influence of Aggregate Grading

(1) Rutting evaluation

The results of wheel tracking tests are presented in **Figures 16** and **17** for standard and high-pressure conditions, respectively.

Figure 16 indicates that aggregate grading plays a significant role in providing asphalt concrete with resistance to permanent deformation; that is, the SPs and SA have lower rutting potential than SMA and DGA. Among the Superpave asphalt concretes, the coarser grading (SP-A) shows lower rutting potential than the fine grading (SP-B). **Figure 17** shows that under high tire pressure SA has better resistance to rutting than other asphalt concretes, followed by SMA and SP-A; SA emphasizes stone-to-stone contact. This also means that grading has a very important influence on rutting susceptibility.

Table 14 Influence of asphalt on properties of asphalt concretes

Item	Straight 60/80	Modified
Dynamic stability (cycles/mm)	1286	7875
Dynamic stability under high-pressure wheel (cycles/mm)	231	2250
Stripping ratio (%)	8.7	0
Strength (MPa)	6.997	8.927
Strain at failure ($1x10^{-3}$)	5.54	6.04
Stiffness (MPa)	1541.1	1478
Permeability coefficient ($1x10^{-7}$ cm/sec)	1.57	2.71
Abrasion loss (cm^2)	0.29	0.20

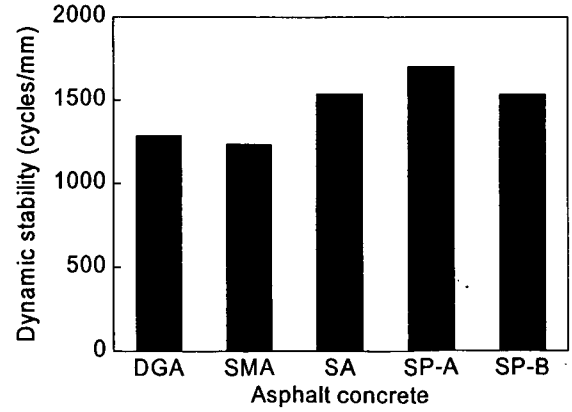

Figure 16 Dynamic stability under standard conditions

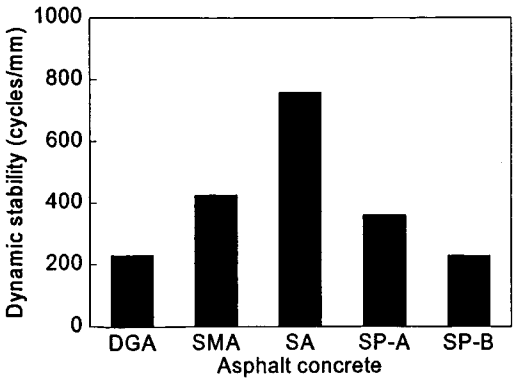

Figure 17 Dynamic stability under high-pressure conditions

(2) Moisture damage evaluation

The results of immersed wheel tracking tests are presented in **Figure 18**, showing that the SPs and SA have low stripping ratios. This is expected, due to the thicker binder film in these gradings, which provides improved adhesion between aggregate particles and thus protection against moisture damage. On the contrary, SMA and DGA have high stripping ratios, for SMA is related to large air voids and DGA to grading.

(3) Low-temperature cracking evaluation

The results of low-temperature flexural tests are presented in **Figures 19, 20** and **21**. From these figures, it can be seen that SMA and SA have higher strength and failure strain, and lower stiffness, than other asphalt concretes. Therefore, asphalt concretes containing these aggregate gradings should offer better resistance to low-temperature cracking. DGA and the SPs show no significant difference in resistance to low temperature cracking.

(4) Water permeability evaluation

The permeability of the asphalt concretes is shown in **Figure 22**.

Higher permeability is exhibited by SMA, SA, and SP-A. This is due to the fact that they contain larger percentages of coarse aggregate, which might result in larger air voids formed by the aggregate skeleton with stone-to-stone contact.

(5) Abrasion evaluation

The results of the raveling tests are presented in **Figure 23**, showing that SA and SP-A exhibit lower abrasion loss than others.

In summary, the test results show that stone asphalt concrete and the Superpave asphalt concretes (with both aggregate gradings) are superior in all properties to other asphalt concretes. Therefore, aggregate grading is recognized as the dominant factor leading to improved resistance of asphalt concretes to both rutting and low-temperature cracking.

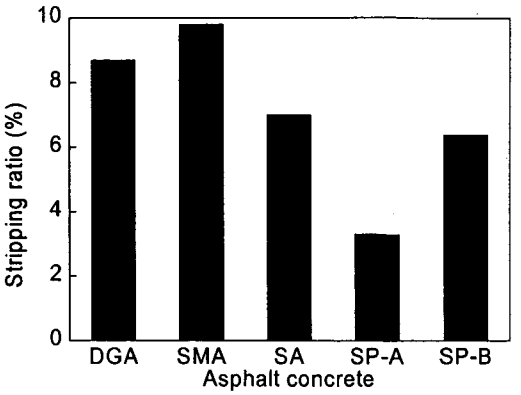

Figure 18 Stripping ratio

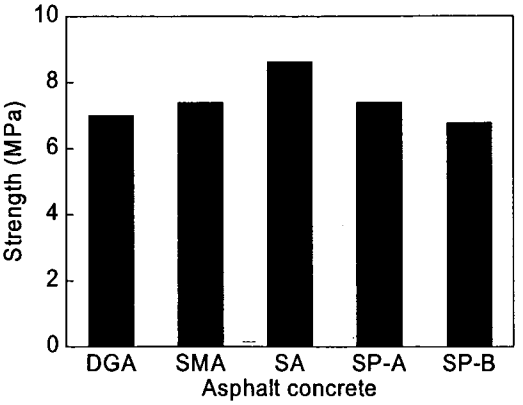

Figure 19 Strength at low temperature

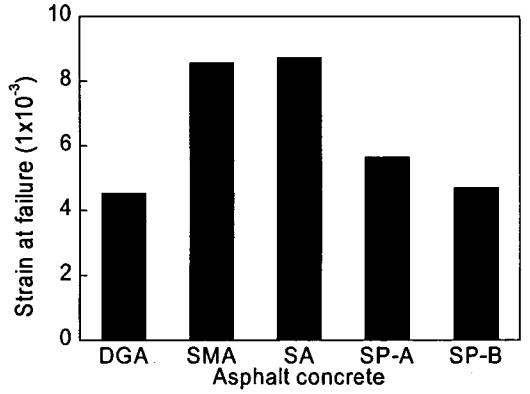

Figure 20 Failure strain at low temperature

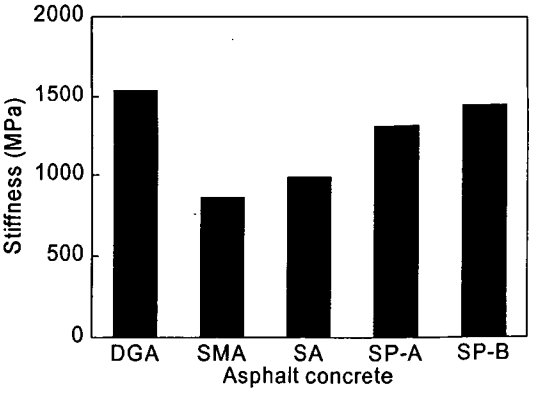

Figure 21 Stiffness at low temperature

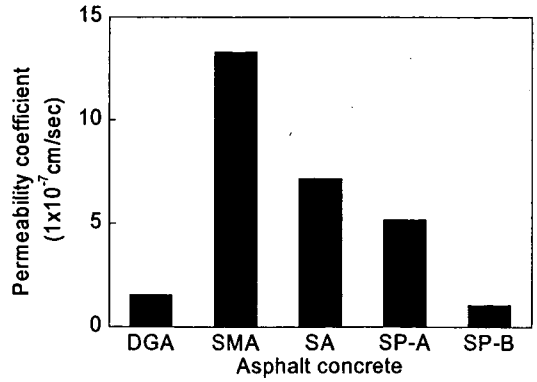

Figure 22 Permeability coefficient

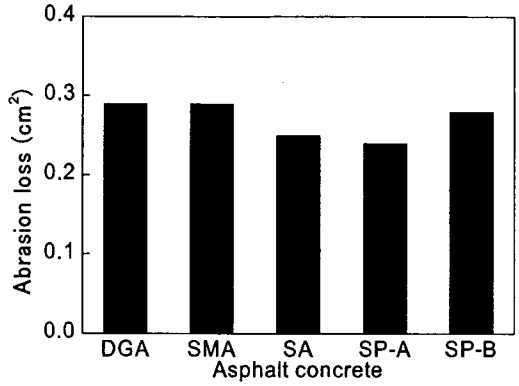

Figure 23 Abrasion ratio

3.6 Influence of Compaction Effort

In order to evaluate the influence of varying compaction effort on the performance of asphalt concretes, three different levels of compaction effort were tested, as shown in **Table 15**. Two hammers were used and their drop heights were adjusted to obtain the specified compaction; that is, the standard (A), and 1.5 (B and C) and 2 times (D) the standard effort.

Representative results of Marshall tests for DGA are shown in **Figures 24, 25,** and **26** for air void volume, stability, and flow, respectively. The relationships between asphalt content and these characteristics are greatly influenced by compaction effort: air void volume decreases and stability increases with greater compaction effort at the same asphalt content. The lower asphalt content is enough to satisfy the specifications when higher compaction effort is used, in comparison with the case of standard compaction effort. In contrast, the relationship between asphalt content and flow does not vary in any specific way with compaction effort.

Wheel tracking test results show that dynamic stability increases with compaction effort in both standard and high tire pressure cases (**Figure 27**). In addition, immersed wheel tracking test results show that the stripping ratio decreases when the compaction effort is greater (**Figure 28**). As the properties of asphalt concrete are improved with the greater hammer mass for the same compaction effort, increasing the roller mass would lead to improved quality.

Table 15 Compaction method

ID	Hammer mass (kg)	Drop height (cm)	Blows (times)	Compaction effort kg·cm)
A	4.5	45.7	75	15424
B	4.5	45.7	113	23238
C	10.2	45.7	50	23238
D	10.2	45.7	66	30765

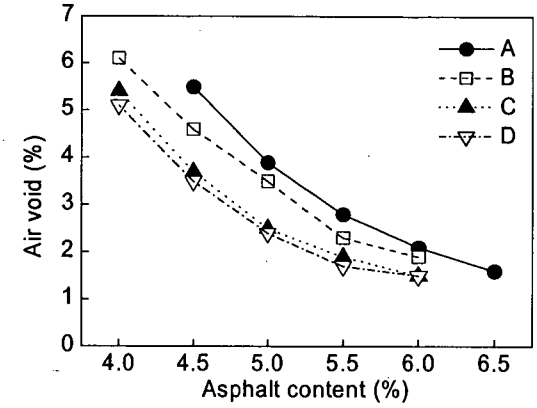

Figure 24 Change in air void volume with compaction effort

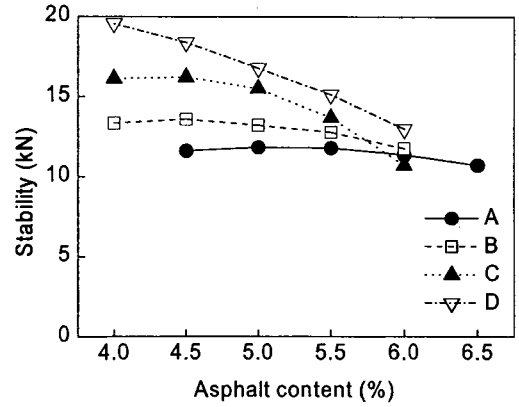

Figure 25 Change in stability with compaction effort

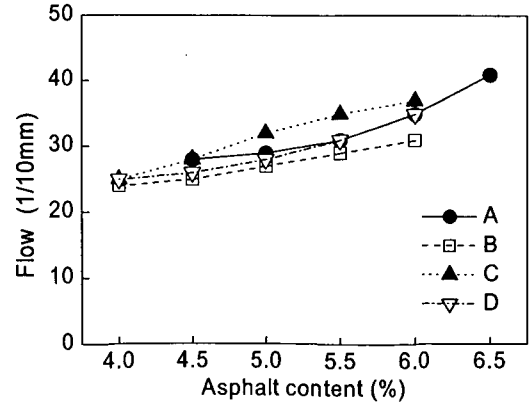

Figure 26 Change in flow with compaction effort

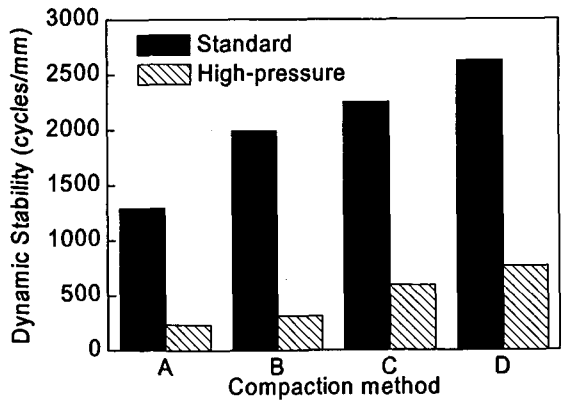

Figure 27 Dynamic stability and compaction effort

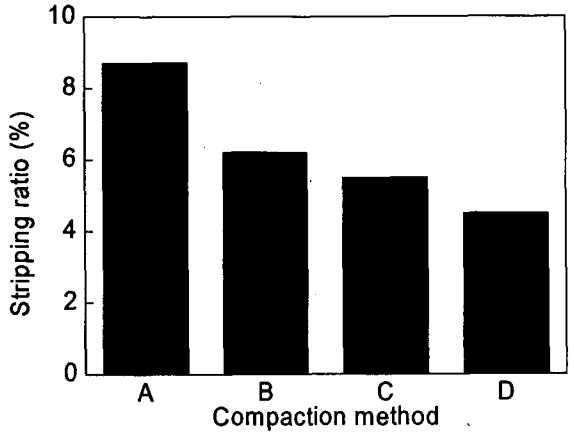

Figure 28 Stripping ratio and compaction effort

3.7 Summary

On the basis of the laboratory test results, the following conclusions can be drawn:

1) Asphalt concrete made with the modified asphalt has better dynamic stability than that made with conventional straight asphalt, and also has lower susceptibility to cracking at low temperatures as well as lower abrasion loss.
2) Aggregate grading greatly influences the resistance of asphalt concrete to rutting at high temperatures and to cracking at low temperatures. Stone asphalt concrete and Superpave asphalt concrete both exhibit improved performance for airport pavements.
3) As the compaction effort increases, the air void ratio of the asphalt concrete is reduced and stability increases. Increasing the compaction effort gives asphalt concrete greater resistance to both rutting and stripping.

4. EVALUATION OF ASPHALT PAVEMENT GROOVE DURABILITY

4.1 Introduction

The surface texture of a newly laid asphalt pavement is usually quite smooth due to the rolling process carried out to meet the specifications. To achieve the moderate degree of surface friction required, several methods are used, including treatment with special surface materials such as an open-graded friction course or a chip seal, surface grooving, and others[9]. Of these methods, grooving is becoming the norm for runways worldwide. The standard configuration specified by the Federal Aviation Administration has been adopted in Japan; that is, 6 mm in depth, 6 mm in width, and 38 mm center-to-center spacing[10].

With aircraft becoming larger and operational frequencies increasing, deterioration of the grooves has become a problem; loss of groove volume occurs at high temperatures and asphalt concrete wear takes place at low temperatures. An early investigation[11] revealed that asphalt concrete may have insufficient durability for heavy-duty loading, as a result of several factors including aggregate and asphalt properties, asphalt content, and environmental conditions.

4.2 Materials and Mixture Design

The materials used in this study were as follows: coarse aggregate (S-4, S-5, S-6, and S-7), fine aggregate (screening, fine sand, and coarse sand), filler, straight asphalt (40/60, 60/80, and 80/100 penetration grade), and modified asphalt (types I and II). The types of asphalt concrete are shown in **Table 16**.

Table 16 Types of asphalt concrete

No.	Asphalt*	Aggregate	
		Maximum size (mm)	Grading
1	S 60/80	13	Usual
2	S 60/80	13	Coarse
3	S 60/80	20	Usual
4	S 40/60	13	Usual
5	S 80/100	13	Usual
6	M-I	13	Usual
7	M-II	13	Usual
8	M-II	20	Usual

*S, M-I, and M-II denote straight, modified (I), and modified (II), respectively.

According to the common specifications for airport civil engineering work[11], the asphalt concrete compositions were designed according to the Marshall stability test method. The results are summarized in **Table 17**. The properties of these mixtures, such as air void volume, stability, flow, and residual stability, satisfied the specified values.

Table 17 Compositions and Marshall test results

Items		No.							
		1	2	3	4	5	6	7	8
Aggregate content (%)	S-4								
	S-5			15.0					15.0
	S-6	37.5	31.0	30.0	37.5	37.5	37.5	37.5	30.0
	S-7	22.0	24.0	13.0	22.0	22.0	22.0	22.0	13.0
	Screening	11.5	13.0	12.0	11.5	11.5	11.5	11.5	12.0
	Coarse sand	17.0	15.0	17.0	17.0	17.0	17.0	17.0	17.0
	Fine sand	6.0	11.0	7.0	6.0	6.0	6.0	6.0	7.0
	Filler	6.0	6.0	6.0	6.0	6.0	6.0	6.0	6.0
Asphalt content (%)		5.6	5.8	5.3	5.6	5.6	5.6	5.6	5.3
Density (g/cm^3)		2.39	2.37	2.40	2.39	2.39	2.39	2.38	2.40
Air void (%)		3.0	3.3	3.0	3.0	2.9	3.0	3.2	2.8
VFA (%)		81.1	80.0	80.2	81.3	81.7	81.1	79.9	81.6
Stability (kN)		12.2	12.2	11.9	11.9	10.8	14.6	13.3	16.4
Flow (1/100 cm)		28	28	30	33	27	36	37	34
Retained stability (%)		84.4	94.2	86.3	85.6	83.0	85.1	94.7	89.4

4.3 Sample Preparation and Test Method

(1) Sample preparation

The asphalt concrete was compacted into a 300 mm square by 50 mm deep mold to a compaction degree of 98% or more for the wheel tracking tests, and into a mold measuring 150 mm wide, 400 mm long, and 50 mm deep for the raveling test.

Grooving is added a specific period, generally two months or more, after pavement construction. In this study, accelerated aging and accelerated tire loading are used to simulate actual conditions. Accelerated aging[12] was carried out in an oven at a high ambient temperature of 60°C to accelerate the process of asphalt concrete aging through the oxidation reaction (**Figure 29**). The aging procedure was conducted as follows:

1) Remaining air was discharged from the oven using a vacuum pump.
2) The oven was filled with oxygen under pressure.
3) Asphalt concrete specimens were sealed in the oven for six hours (one cycle).
4) Steps 1) through 3) were repeated.

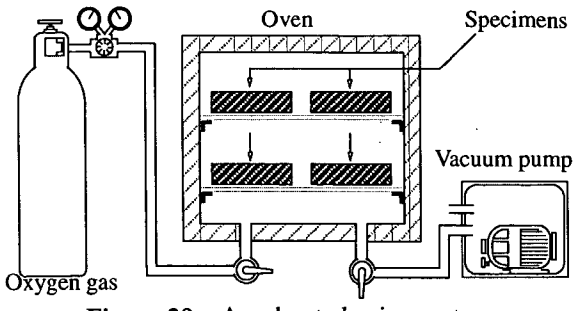

Figure 29 Accelerated aging system

After each cycle of the aging process, accelerated wheel loading was carried out on some specimens with a weighted wheel; the tired wheel provided a contact pressure of 320 kPa and 700 back and forth cycles were applied with a transverse shift. **Figure 30** shows the tired wheel, and **Table 18** its specifications. **Table 19** shows the various acceleration conditions. Assuming that accelerated aging for twelve hours corresponds to four weeks of actual aging[12], this study covers the period from construction to six months. The number of aircraft passes is assumed to be about 50 per day, so 1,400 cycles are used to represent four weeks.

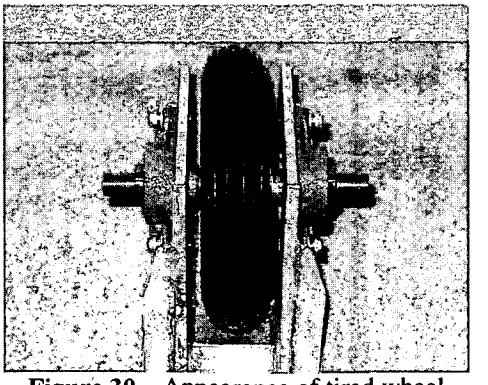

Figure 30 Appearance of tired wheel

Table 18 Specifications of tired wheel

	Specification
Outer diameter (mm)	202
Width (mm)	54
Air pressure (kPa)	200
Load (N)	700
Contact pressure (kPa)	320

Table 19 Acceleration conditions

Case	Aging (hours)	Tracking (cycles)
a-1	12	-
a-2	24	-
a-3	36	-
a-4	72	-
b-1	12	1,400
b-2	24	2,800
b-3	36	4,200
b-4	72	8,400

After completion of the specified curing procedures, grooves were cut using a cutter with diamond heads. Seven grooves with a width and depth of 6 mm were cut transversely at a spacing of 38 mm for both tests. **Figure 31** shows a grooved specimen prepared for the raveling test.

(2) Test method

The wheel tracking test aims to evaluate the loss of groove volume at high temperatures, whereas the raveling test is used to examine material wear at low temperatures, as already noted. Both procedures generally followed the standard methodology[13].

a) Wheel tracking test

Table 20 gives the test conditions. To evaluate the results, the loss of groove volume was calculated using **Equation 1**.

$$LV = \frac{a_0 - a_i}{a_0} \times 100 \ (\%) \qquad (1)$$

where,

LV: loss of groove volume,

a_0: groove volume at start of test,

a_i: groove volume at time of measurement.

Figure 31 Grooved specimen

Table 20 Conditions for wheel tracking test

	Conditions
Temperature	40°C
Wheel type	Solid tire
Wheel size	200 mm deep, 50 mm wide
Load	700 N
Tracking rate	42 cycles/min

b) Raveling test

Table 21 gives the test conditions. To evaluate the results, the change in groove volume was calculated using **Equation 2**.

$$CV = \frac{a_i}{a_0} \times 100 \ (\%) \qquad (2)$$

where,

CV: change in groove volume,

a_0: groove volume at start of test,

a_i: groove volume at time of measurement.

Table 21 Conditions for raveling test

	Conditions
Temperature	0°C
Chain material	Solid
Number of chains	10 links × 12
Number of wheel rotations	200 rpm
Number of specimen moves	66 cycles/min

4.4 Test Results and Discussion

The influence of the three factors studied on groove stability, as determined from the tests, is described below.

(1) Aggregate grading

Asphalt concretes made using the same asphalt are compared so as to evaluate the influence of aggregate grading. **Figures 32** and **33** show the loss of groove volume at high temperature and change in groove volume at low temperature, respectively, for the case of straight asphalt 60/80. While asphalt concrete containing larger aggregate shows smaller loss early on in the wheel tracking test, in the end there is little difference in durability between the various gradings. Unlike the former study, asphalt concrete made with a coarse aggregate grading does not exhibit better performance (comparing the results for aggregates No. 1 and No. 2). Thus aggregate grading may have no effect on groove volume change at low temperatures.

Figure 34 shows the influence of maximum aggregate size on volume loss at high temperatures in the case of modified asphalt. There is no clear trend, as in the case of straight asphalt.

(2) Asphalt

Asphalt concretes made using five different asphalt types were evaluated for the case of aggregates with maximum size of 13 mm and the usual grading. **Figure 35** shows how volume loss changes with the number of wheel tracking cycles at high temperature. These asphalt concretes are of two types: those made with straight asphalts and those made with modified asphalts. The latter exhibit better resistance to volume loss under repeated loading, so asphalt viscosity might be a useful

indicator of groove durability.

Volume change at low temperatures is unaffected by asphalt type, as shown in **Figure 36**.

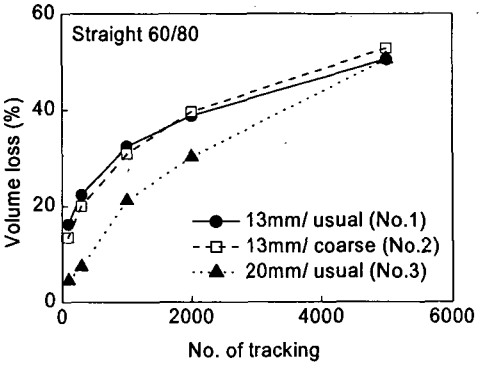

Figure 32 Aggregate grading and volume loss

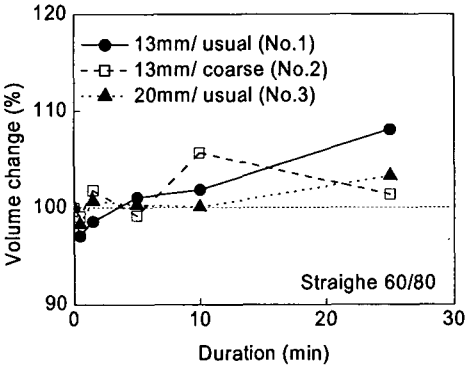

Figure 33 Aggregate grading and volume change

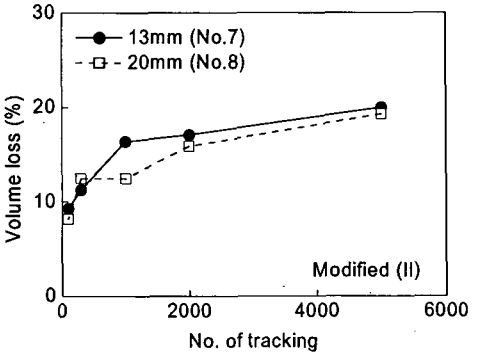

Figure 34 Aggregate size and volume loss

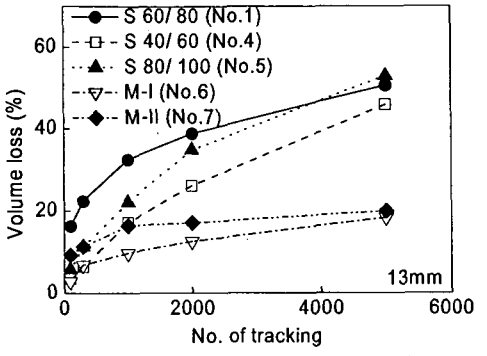

Figure 35 Asphalt type and volume loss

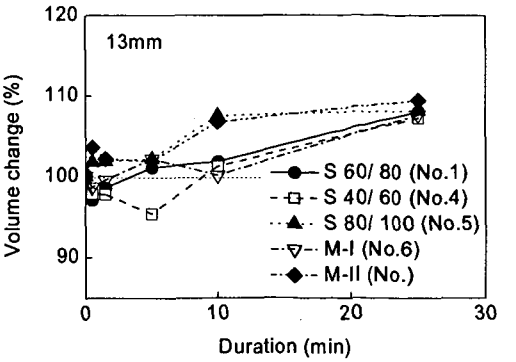

Figure 36 Asphalt types and volume change

(3) Curing method

To clarify the influence of curing prior to groove cutting, specimens with different accelerated curing conditions were tested. These specimens were conventional asphalt concretes made of straight 60/80 asphalt and well-graded aggregates with a maximum size of 13 mm.

Figure 37 shows the results for specimens without traffic loading. After 72 hours of curing, the performance of specimens is improved. On the contrary, loading has an enormous effect on the resistance of asphalt concrete to volume loss at high temperatures, as shown in **Figure 38**.

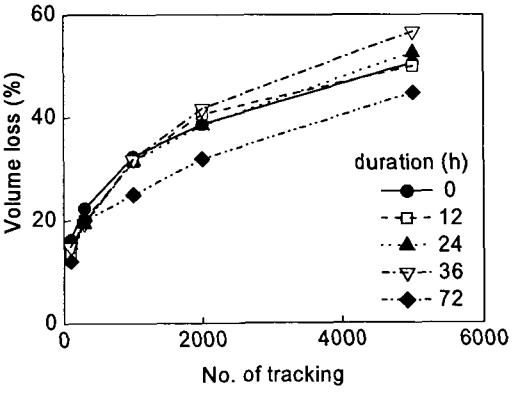

Figure 37 Volume loss without tracking

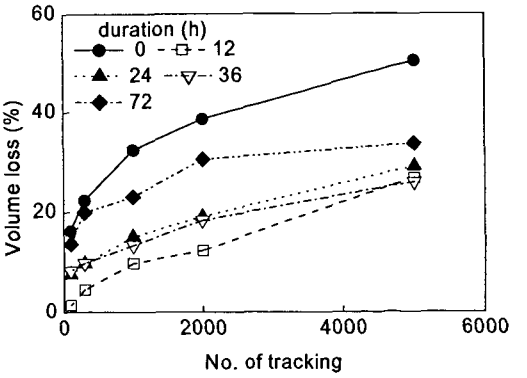

Figure 38 Volume loss with tracking

Table 22 Properties of recovered asphalt

	Without	a-1	a-2	a-3	a-4	b-1	b-2	b-3	b-4
Penetration at (25 C,1/10mm)	48	49	45	45	46	44	44	41	43
Softening point (C)	51.5	52	52	52.5	52.5	52.6	53	53.5	53
Ductility (15 C, cm)	42	41	31	16	13	16	15	11	13
Viscosity (60 C, Pa s)	3900	4000	4200	4600	4500	4700	5000	5900	4900
Density (g/cm^3)	1.042	1.043	1.043	1.042	1.043	1.044	1.044	1.044	1.045

Table 23 Evaluation of test methods for low-temperature cracking

Test method	Properties measured	Simulation of field conditions	Application of test results to mechanistic model
TSRST	Tensile strength and fracture temperature	Yes	Direct
Thermal contraction	Thermal contraction coefficient	Yes	Indirect
Indirect tension	Tensile stress and strain	No	Indirect
Direct tension	Tensile stress and strain	No	Indirect
Bending	Tensile stress and strain	No	Indirect
Bending creep	Tensile stress and strain	No	Indirect
J-integral	Energy release rate	No	Indirect

Table 24 Properties of asphalts used

		Asphalt type			
		A	B	C	D
Penetration (1/10mm)	25 °C	81	75	93	91
	15 °C	25	33	43	36
	5 °C	8	10	17	14
Ductility (cm)	25 °C	72	22	>100	>100
	5 °C	4.5	>100	13	11
Softening point (°C)		46.8	51.3	48.8	46.7
Density (g/cm^3)		0.996	0.958	1.021	1.005
PI		-0.854	0.150	1.21	-0.551
PR (%)		10.125	7.5	5.47	6.5
Fraass breaking point (°C)		-11	-14.9	-22.7	-16.5

Table 22 shows the properties of the asphalt recovered from tested asphalt concretes. The viscosity of the asphalt increases with curing period, especially in the case of loaded specimens.

4.5 Summary

The results of these tests can be summarized as follows: a) Neither grading nor maximum aggregate size have much effect on groove durability at high temperatures; b) Modified asphalt greatly improves durability at high temperature; c) Curing period has a performance-improving effect, whereas loading has a large effect.

Based on these results, modified asphalt is recommended for use in both new pavement construction and for overlay work if sufficient curing period cannot be secured. Straight asphalt is also applicable to both types of work, but especially for overlays when a longer period is available before groove cutting. To verify the results of this study and to specify curing periods for actual implementation, field studies must be conducted.

5. SIMPLE TEST FOR EVALUATION OF ASPHALT MIXTURE RESISTANCE TO LOW-TEMPERATURE CRACKING

5.1 Introduction

The deterioration of asphalt pavements as a result of low-temperature cracking, which is attributed to tensile stresses induced when temperatures drop extremely low, is a significant and costly problem throughout the world. When the pavement cools, it tends to contract. However, friction between the asphalt concrete layer and the base course inhibits contraction and tensile stress builds up. As a result, micro-cracks develop at the pavement surface after repeated temperature fluctuations. These then penetrate into the asphalt concrete layer, and often reach to the bottom of the layer[14),15)].

reach to the bottom of the layer[14),15)].

A number of test methods have been used to evaluate this type of thermal cracking in asphalt concrete, as summarized in **Table 23**[14)]. These methods can be divided into three types:

1) Thermal stress restrained specimen tests (TSRST) and thermal contraction tests, which simulate actual conditions in the field.
2) Indirect tension, direct tension, bending, and bending creep tests, which yield the low-temperature stress-strain characteristics of the asphalt mixture.
3) J-integral tests, which yield fracture mechanics parameters such as the energy release rate.

With the exception of the TSRST and J-integral tests, these tests are relatively easy to implement. The TSRST test is difficult because it entails gluing the specimen to a platen, while the J-integral test moderately difficult because the specimen must be notched and the rate of crack propagation monitored. Procedures for the other tests are well established and documented. The equipment associated with the indirect tension, direct tension, and bending tests is routinely used in many laboratories, whereas that for bending creep, thermal stress, and thermal contraction is not routinely available.

In this study, four different methods — TSRST, bending test, bending creep test, and J-integral test — are used to evaluate four different kinds of performance of asphalt mixtures at low temperatures, and then a simple test method is suggested based on the results.

5.2 Material Properties

Four different asphalts and one type of limestone aggregate were used in the study; the three asphalts, derived from different crude oils, are identified as A, C, and D. Asphalt B is asphalt A modified with SBR. The properties of these asphalts and the aggregate are summarized in **Table 24** and **Table 25**, respectively. A medium aggregate grading was used in preparing the asphalt mixtures, as shown in **Table 26**.

The asphalt mixtures were designed using the 75-blow Marshall method, and the optimum asphalt content for all the asphalts was fixed at 4.0%.

Based on a consideration of PR, ductility at 5°C, and the Fraass breaking point of asphalts, it is possible to rank asphalts as A, B, D, and C from the viewpoint of performance at low temperatures.

Table 25 Properties of aggregate

Item	Measured value
Apparent density (g/cm^3)	2.763
Crash value (%)	18.5
LA abrasion value (%)	10.2

Table 26 Aggregate grading

Sieve size (mm)	Percent passing (%)	Specification limits (%)
19	100	100
16	97.5	95-100
13.2	82.5	75-90
9.5	68	58-78
4.75	52.5	42-63
2.36	41	32-50
1.18	29.5	22-37
0.6	22	16-28
0.3	16	11-21
0.15	11	7-15
0.074	6	4-8

5.3 Experimental Procedure

(1) TSRST

In the TSRST, the stress required to confine deformation of specimen is measured while the temperature is reduced; the thermally induced stress gradually increases as temperature falls until the specimen fractures, as shown in **Figure 39**. The stress reaches its maximum value at the failure point, which corresponds to the fracture strength at that temperature. The slope of the thermally induced stress curve, ds/dT, increases until it reaches a constant and maximum value. The curve can be divided into two paths at the transition temperature; thermally induced stress relaxes if the temperature does not fall below the transition temperature, but does not if the temperature falls lower.

Asphalt concrete specimens, 50mm wide, 50mm high, and 250mm long, were glued to end platens with an epoxy compound. Specimens were placed in an environmental cabinet after the epoxy had cured, and cooled at a rate of 10°C/h. Before testing, all gauges including the LVDT were fixed in place, and a computer was used to correct the platen position and record all required data until fracture.

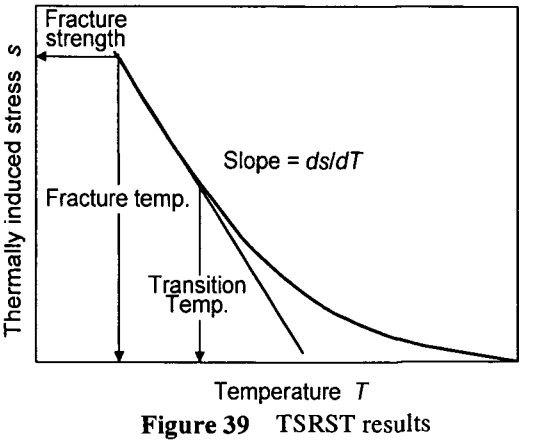

Figure 39 TSRST results

(2) Bending test at low temperature

A three-point bending test was used to determine the stiffness, strength, and strain at failure of the asphalt mixture at low temperatures. The concept of strain energy density was also adopted to evaluate the low-temperature performance of the asphalt mixture; this can be calculated by integrating the area under the stress-strain curve, as shown in **Figure 40**.

$$U = \int_0^{\varepsilon} \sigma \cdot d\varepsilon \qquad (3)$$

where, U: strain energy density; σ: stress; and ε: strain.

Specimens were the same size as in the TSRST. The test temperature was 0°C and the loading rate was 1mm /min.

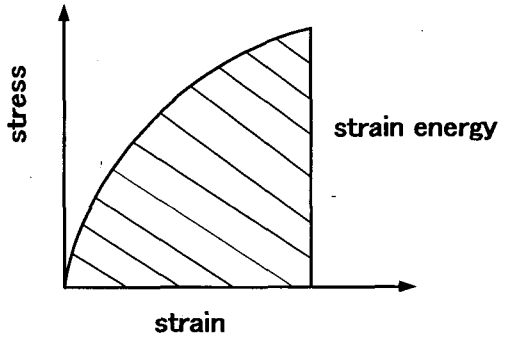

Figure 40 Strain energy density concept

(3) Bending creep test

A bending creep test was conducted by applying a constant load to the specimen and recording the resulting deformation with time. Specimens measuring 30, 35, and 250mm in width, height, and length, respectively, were used, and a constant load of 1MPa was applied at 0°C. The resulting creep curve can, as usual, be divided into three distinct stages as shown **Figure 41**.

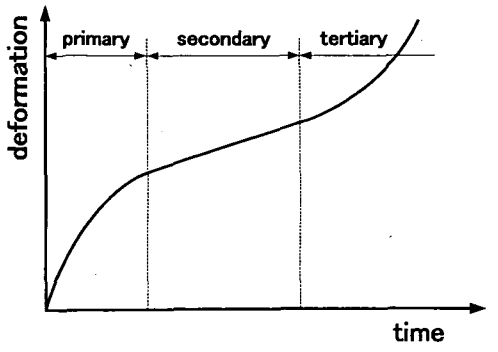

Figure 41 Creep curve of asphalt mixture

a) Primary stage

Upon the initial loading, deformation rapidly increases, indicating a very high rate of deformation.

b) Secondary stage

The rate of deformation during the secondary stage is essentially constant. This rate was selected as an index of the deformation performance of the asphalt mixture; a higher rate of deformation indicates better anti-cracking performance.

c) Tertiary stage

In this final stage, the rate of deformation tends to accelerate until complete failure takes place. This stage is usually associated with crack formation.

The creep rate is calculated in this test as follows:

$$\varphi = (D_{t2} - D_{t1})/(t_2 - t_1) \qquad (4)$$

where, φ: creep rate and D_{t1}, D_{t2}: deformation at time t_1, t_2, respectively.

(4) J-integral test

The J-integral test for determining fracture toughness is based on the principles of elasto-plastic fracture mechanics. The J-integral is a path-independent measure of the energy required to initiate a crack at a notch tip[16]. Experimentally, the critical J-integral fracture toughness is determined in a test using notched beams in a three-point bending configuration, as shown in **Figure 42**.

The fracture toughness, J_{Ic}, is given by the following equation:

$$J_{Ic} = -1/b \frac{du}{da} \qquad (5)$$

where, b: beam width; u: total strain energy to failure; and a: notch length.

The test was performed at a constant loading rate of 0.5 mm/min. and at 0°C.

5.4 Results and Analysis

(1) TSRST

The results of the thermal stress restrained specimen test are given in **Table 27**.

In terms of fracture temperature and transition temperature, the asphalts can be ranked as A, B, D, and C. This agrees with the ranking based on the physical properties of asphalts. However, the ranking according to the fracture stress and curve slope differs from this. This means that the fracture temperature and transition temperature are primarily affected by asphalt type followed by aggregate type.

(2) Bending test

The bending test results for the asphalt mixtures at 0°C are given in **Table 28**.

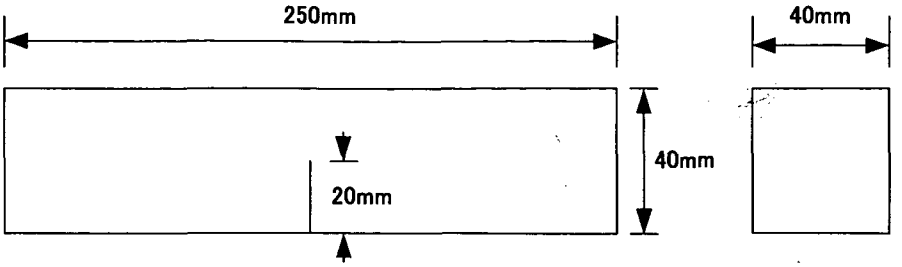

Figure 42 Specimen for J-integral test

Table 27 TSRST results

Asphalt type	Fracture temperature (°C)	Fracture stress (MPa)	Transition temperature (°C)	Slope (MPa/°C)
A	-22.7	4.83	-17.4	3.404
B	-26.9	6.06	-22	4.471
C	-34.4	5.88	-28.1	4.495
D	-29.4	4.25	-23.8	2.656

Table 28 Bending test results at 0°C

Asphalt type	Strength (MPa)	Strain at failure ($1x10^{-6}$)	Stiffness (MPa)	Strain energy density (kJ/m^3)
A	9.707	955	10374	4370
B	9.180	1152	7969	5203
C	10.097	1212	8331	6949
D	9.385	1294	7252	6080

Table 29 Results of bending creep test at 0°C

Asphalt type	Creep rate ($1x10^{-6}$/s)
A	44.6
B	36.9
C	112
D	103.2

In this test, the ranking of the asphalts depends on the indicator chosen, though asphalts C and D are superior to A and B on the whole. Among these values, strain energy density might make a good indicator, as it gives the same rankings as the physical properties of asphalt and fracture temperature in the TSRST. With greater asphalt strength, higher strain at failure and lower stiffness are expected at low temperature, so in this sense strain energy density offers the advantage that it takes into account both stress and strain.

(3) Bending creep test

The results of the bending creep test for asphalt mixtures at 0°C are given in **Table 29**. From the creep rate, the ranking of asphalts from lowest to highest is B, A, D, and C.

Since the level of stress influences the creep characteristics of asphalt mixtures[17], various stress levels were applied in this test. The results are described in **Figure 43**. This represents the effect of stress level on the creep rate of asphalt mixtures at low temperature. The accumulated strain increases with stress level, and it changes dramatically when the stress exceeds 1MPa.

In **Figure 44**, creep rates are plotted against the ratio of applied stress to strength. It is particularly interesting that the transition stress here is close to 10% of the fracture stress. A future task is to determine a suitable standard stress level for use in this low-temperature creep test.

(4) J-integral test

The results of the J-integral test are given in **Table 30**. The ranking of asphalts according to fracture toughness is A, B, D, and C.

5.5 Regression of Fracture Temperature against Other Indicators

Regressions between the fracture temperature as measured in the TSRST and indicators measured in the other tests are shown in **Figures 45, 46, 47, 48, 49, 50** for four asphalt mixtures. A particularly high regression coefficient of 0.98 is obtained between fracture temperature and strain energy density from the bending test. Good regression coefficients are also obtained for other indicators: 0.89 for fracture temperature against J_{Ic} from the J-integral test; and 0.71 between fracture temperature and creep rate from the bending creep test.

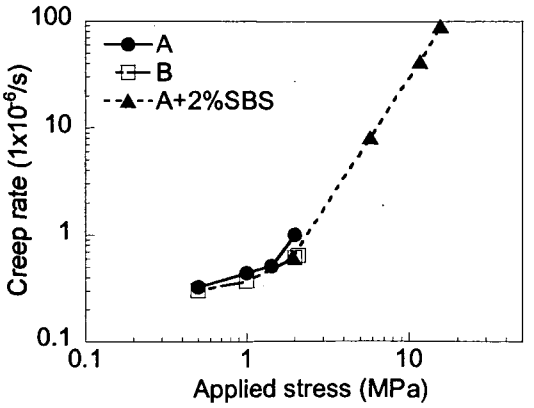

Figure 43 Applied stress and creep rate

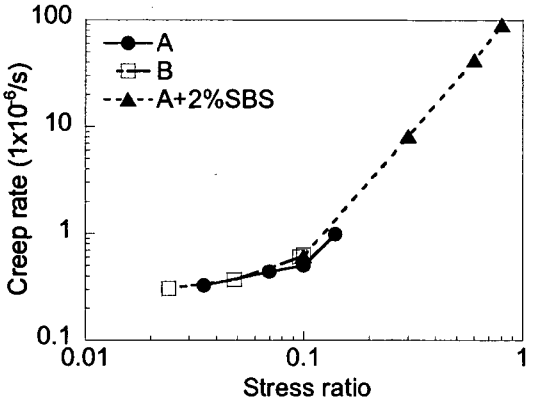

Figure 44 Stress ratio and creep rate

Table 30 J-integral test results at 0°C

Asphalt type	J_{Ic} (kJ/m^2)
A	355.84
B	437.13
C	543.17
D	522.32

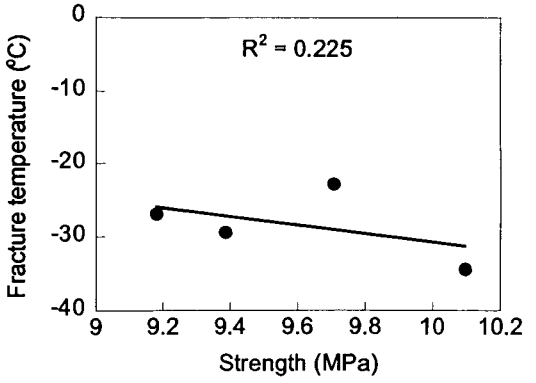

Figure 45 Fracture temperature and strength in bending test

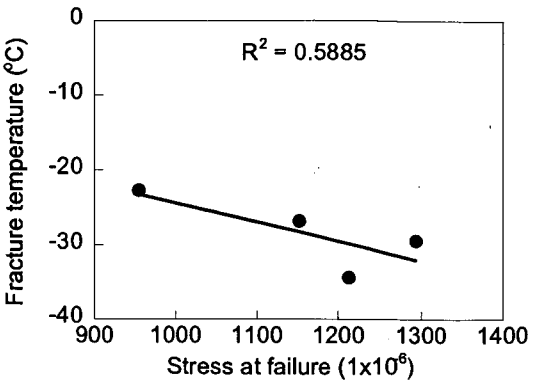

Figure 46 Fracture temperature and failure strain in bending test

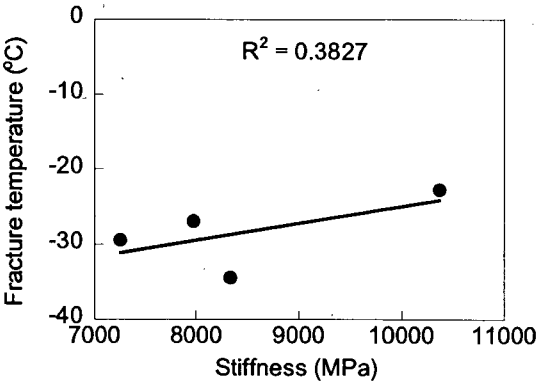

Figure 47 Fracture temperature and stiffness in bending test

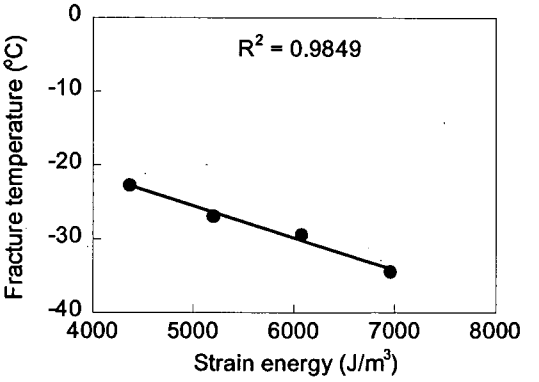

Figure 48 Fracture temperature and strain energy density

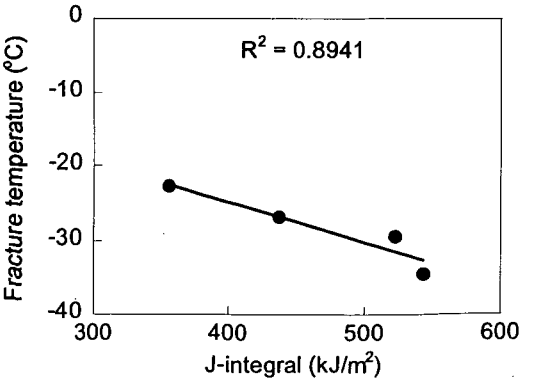

Figure 49 Fracture temperature and J_{Ic}

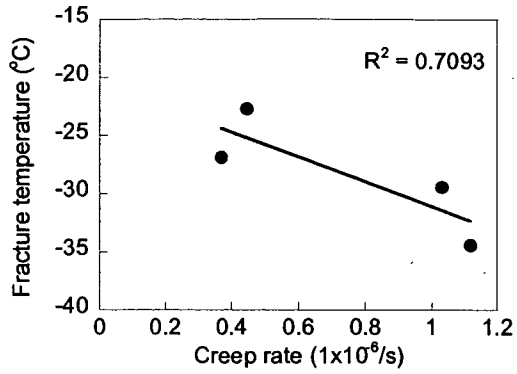

Figure 50 Fracture temperature and creep rate

5.6 Summary

Thermal stress testing of restrained specimens offers an effective means of evaluating the anti-cracking properties of asphalt mixtures at low temperatures, since the results, and especially the transition temperature, agree quite well with the properties of the asphalt. The strain energy as determined in a simple bending test correlates well with fracture temperature obtained from a TSRST, so the bending test could take the place of the TSRST in some situations; the bending test is quick and easy to perform whereas the TSRST is very time-consuming and expensive. In particular, the bending test might best be used as a screening test for different asphalt mixtures.

6. EVALUATION INDICATOR OF ASPHALT MIXTURE RUTTING SUSCEPTIBILITY

6.1 Introduction

Premature rutting of an asphalt pavement can be prevented by proper mix design and production. Increased truck traffic, heavier axle loads, and higher tire pressures are among the factors that have increased the demand for asphalt mixtures that resist rutting. For the purposes of design as well as quality control/assurance, a methodology is needed for accelerated laboratory rutting prediction tests. Laboratory equipment could potentially be used to evaluate rutting susceptibility for design and quality control[18), 19)].

Many methods are used to evaluate the performance of asphalt pavements at high temperatures, including single-axle static and dynamic creep tests, the repetitive creep test, tri-axial static and dynamic creep tests, the simple shear test, the wheel-tracking test, and the full-scale test[20)]. Before a new laboratory testing procedure can be accepted as a more accurate measure of mixture behavior at high temperatures, the laboratory results must be shown to closely correlate with pavement performance in the field. Further, the test method should be simple to use[21)]. Given these basic conditions, laboratory wheel-tracking devices are often the best test methods.

Different wheel-tracking devices and evaluation indicators are used in different countries. They include the French pavement rutting tester (PRT), the Hamburg wheel-tracking device (WTD), the Georgia loaded-wheel tester (GWT and APA), the Japan wheel-tracking device (JWTD), and various other versions of these basic designs. All of these devices are somewhat similar in concept but differ slightly in design and operation[22)].

Table 31 summarizes the similarities and differences among some of these devices. The JWTD is currently used in Asia and the UK, so it is the focus of this study.

The wheel-tracking method specified in the Japan Road Association standard (JHS230-1992) was developed with TRRL in England, and is based on the relationship between the deformation of a slab sample and the number of wheel-tracking cycles (see **Figure 51**). A compacted specimen is held at 60°C and subjected to 42 passes/min. by a special solid rubber tire for 1 hr. The dynamic stability indicator (*DS*) can be defined as follows [13)]:

$$DS = \frac{42 \times 15}{D_{60} - D_{45}} \qquad (6)$$

Where,

DS = dynamic stability (cycles/mm),
D_{60} = tracking depth at 60 min (mm),
D_{45} = tracking depth at 45 min (mm).

In the Japan road standard, *DS* is summarized as in **Table 32**.

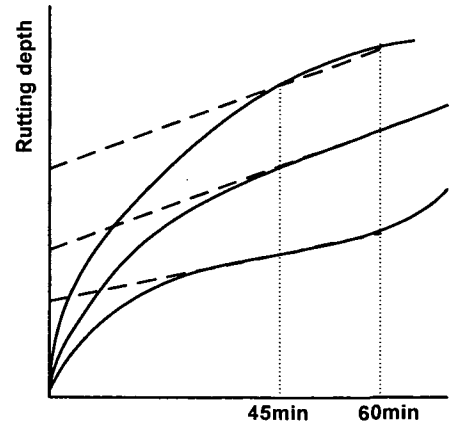

Figure 51 Rutting test curve

Table 31 Testing parameters for several different asphalt mixture wheel-tracking devices

Item	PRT	WTD	GWT	APA	JWTD
Temperature (°C)	60	50	40	5-80	60
Environmental conditions	Hot/dry	Hot/wet	Hot/dry	Hot/wet	Hot/dry
Specimen size, length, width, and thickness (mm)	500, 180, 100	320, 260, 80	300,125, 75	300, 125, 75	300, 300, 50
Wheel type	Pneumatic (500 kPa)	Solid steel	Aluminum wheel on pressurized hose (700 kPa)	Aluminum wheel on pressurized hose (700 kPa)	Solid rubber tire (700 kPa)
Wheel size	Diameter 400 mm, width 90 mm	Diameter 203.5 mm, width 47 mm	Hose diameter 29 mm	Hose diameter 29 mm	Diameter 200 mm, width 50 mm
Load (N)	Up to 5000	Up to 697	Up to 700	Up to 700	Up to 700
Wheel speed (m/s)	1.6	0.33	0.6	0.6	1.47
Maximum cycles	30000	20000	8000	8000	2520
Indicator	Maximum rutting depth 10 mm	Maximum rutting depth 4 mm	Maximum rutting depth 7.6 mm	Maximum rutting depth 5-7 mm	Minimum dynamic stability, 1200 cycles/mm

Table 32 Specifications of the Japan Road Association

Traffic volume category	Truck traffic (one way, volume/day)	Dynamic stability standard (cycles/mm)
Low	Less than 1500	800
Middle	1500–3000	1000
Heavy	3000–15000	1200
Very heavy	More than 15000	3000–5000

Table 33 Binder properties

Penetration (25°C, 1/10 mm)	Ductility (15°C, cm)	Softening point (°C)	Wax content (%)
89	>100	48.5	1.85

The JWTD concept is based upon similar wheel-tracking devices used to study rutting, but some years of use demonstrated that the dynamic stability indicator has some limitations in evaluating the rutting susceptibility of asphalt mixtures in the laboratory.

6.2 Materials

(1) Asphalts

The single source of the asphalt used was the Kelamayi refinery in China; the properties of the asphalt binder are given in **Table 33**.

(2) Aggregates

The properties of the 100% crushed limestone aggregate are given in **Table 34**.

(3) Grading

The aggregate gradings were selected as in **Table 35**.

Based on the specified design obtained by the Marshall test, the final mix results for the A- and B-gradings, as well as the Marshall criteria, are presented in **Table 36** and **Table 37**.

For the AC-13 and AC-20 gradings, the optimum asphalt contents as determined by the Marshall method are 5.5% and 4.8%, respectively. The Marshall test results are given in **Table 38**.

6.3 Sample Preparation and Test Program

Samples with different asphalt contents and different gradations were prepared with a roller-compaction device. Samples measured 300 mm square by 50 mm in thickness. Rutting susceptibility was determined using the Japanese wheel-tracking tester . In this standard test performed at a temperature of 60°C, the 50 mm-thick slab of asphalt mixture was subjected to the rolling load (tire inflation 0.7 MPa) at the specified rate of 42 cycles per minute. Rutting depth was measured periodically over 3000 cycles, and dynamic stability was calculated from the results.

Based on the rutting depth at 3000 cycles, the relative deformation ratio, $\Delta h/H$, is expressed as a percentage: Δh = rutting depth at 3000 cycles (mm) and H = sample thickness (mm).

Table 34 Aggregate properties

Properties	Coarse aggregate	Fine aggregate	Filler
Bulk specific gravity (Dry)	2.709	2.682	-
Bulk specific gravity (SSD)	2.731	2.694	-
Apparent specific gravity	2.750	2.728	2.824
Los Angeles abrasion (% loss)	27.2	-	-
Crush value (% loss)	14.5	-	-

Table 35 Selected aggregate gradings

Sieve size (mm)	Percent passing by weight (%)			
	A-grading	AC-13	B-grading	AC-20
26.5	100	100	100	100
19	100	100	100	95–100
16	95–100	100	90–100	75–90
13.2	75–90	95–100	65–85	62–80
9.5	58–78	70–88	50–70	53–72
4.75	42–63	48–68	30–50	38–58
2.36	32–50	36–53	18–35	28–46
1.18	22–37	24–41	12–26	20–34
0.6	16–28	18–30	7–19	15–27
0.3	11–21	12–22	4–14	10–20
0.15	7–15	8–16	3–9	6–14
0.075	4–8	4–8	2–5	4–8

Table 36 Selected A-grading mix design data

	A1	A2	A3	A4*	A5	A6	Marshall criterion
Asphalt content (%)	4.5	4.8	5.1	5.4	5.7	6.0	-
Stability (kN)	9.5	9.8	10.7	11.6	10.3	9.1	>7.5
Flow (1/10 mm)	20.8	23.7	26.5	29.5	33.2	38.4	20–40
Air void (%)	6.8	5.8	4.8	3.7	3.4	3.1	3–6
Void filled with asphalt (VFA, %)	60.7	66.3	71.5	77.6	79.9	82.0	70–85

*A4 is the optimum asphalt content.

Table 37 Selected B-grading mix design data

	B1	B2	B3	B4*	B5	B6	Marshall criterion
Asphalt content (%)	4.2	4.5	4.8	5.1	5.4	5.7	-
Stability (kN)	8.7	9.2	9.1	8.8	8.5	8.1	>5.0
Flow (1/10 mm)	23.0	24.9	28.1	30.6	33.9	36.2	20–40
Air void (%)	11.8	10.1	8.8	7.5	6.9	6.2	4–10
Void filled with asphalt (VFA, %)	44.2	50.0	55.2	60.8	64.3	68.0	67–75

*B4 is the optimum asphalt content.

Table 38 Marshall test results for AC-13 and AC-20

Grading	Stability (kN)	Flow (1/10 mm)	Air void (%)	VFA (%)
AC-13	13.0	24	3.5	76.4
AC-20	14.2	23	4.3	72.2

6.4 Results and Analysis

(1) Dynamic stability indicator

Figure 52 and **Figure 53** give the rutting depth test results for asphalt mixtures with different asphalt contents.

For A-grading asphalt mixtures, the initial dynamic stability of the A1 asphalt mixture is equal to that of the B-grading B1 mixture. However, after 3000 cycles of loading, the two mixtures have different rutting depths, with the B1 mixture having less rutting. That is, the B1 mixture has better rutting resistance, although the dynamic stability indicator does not match these results.

The dynamic stability of the A3 mixture is 875 cycles/mm, and that of the B4 mixture is 863 cycles/mm. Although these values are very similar, the rutting depth after 3000 cycles of loading shows that the A4 mixture is more stable than the B3 mixture; the same conclusion is reached for the B1 and B4 mixtures.

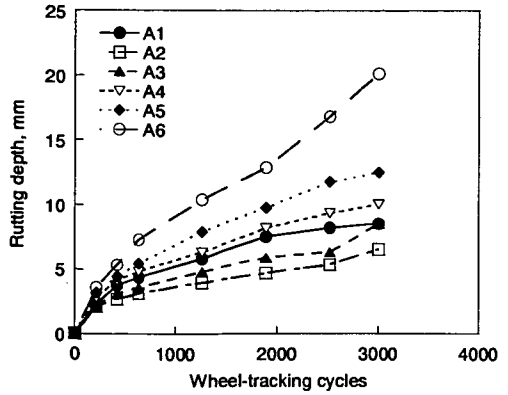

a) A1~A6

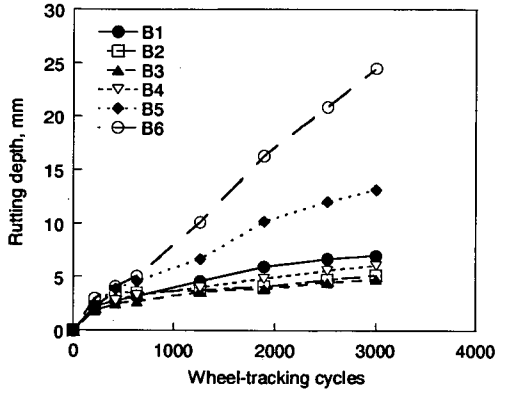

b) B1~B6

Figure 52 Relationship between rutting depth and wheel-tracking cycles

In the wheel-tracking test, the dynamic stability indicator is normally expressed as the number of wheel-tracking cycles against rutting depth between 45 min. and 60 min.; that is, the gradient of the rutting curve in this range. Sometimes it is found that the gradients are very similar, but the rutting depths are significantly different (see **Figure 58**). This figure shows that rutting curves fall into three categories (upward protruding type, straight line type, and reverse curvature type). As the number of wheel-tracking cycles increases, the upward protruding and straight line curves may evolve into the reverse curvature type. Rutting depth can rise significantly, but the slope of the curve between 45 and 60 min. remains unchanged.

From the FHWA-RD-99-204 test data [23] (see **Table 39**), it is seen that there is a significant difference between dynamic stability and rutting depth. When the slab thickness is 100 mm, the dynamic stability of asphalt mixtures with asphalts AC-5, AC-10, and AC-20 is very similar, but rutting depth varies somewhat.

In the wheel-tracking test, the accuracy of deformation measurements influences the dynamic stability values; the results are shown in **Table 40**.

From this table, it can be seen that dynamic stability varies over a wide range while deformation varies only slightly. In particular, if the deformation is less than 0.01

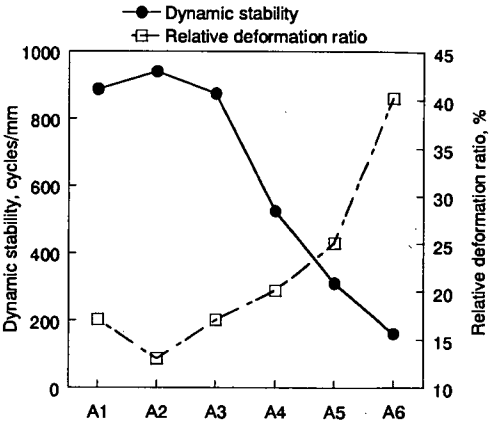

a) A1~A6

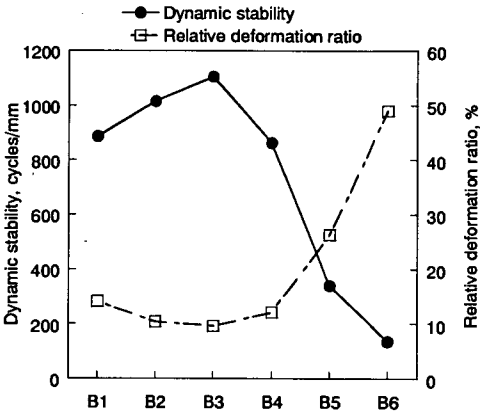

b) B1~B6

Figure 53 Comparison of dynamic stability and relative deformation ratio

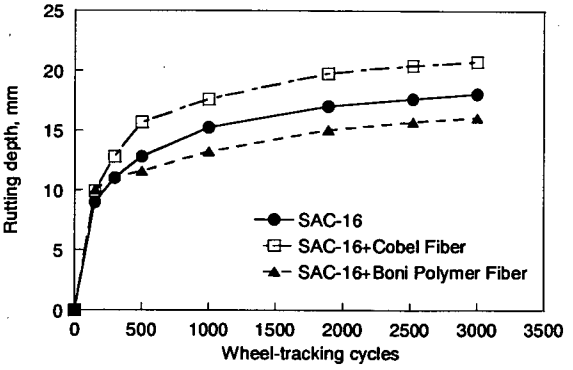

Figure 54 Relationship between rutting depth and wheel-tracking cycles for SAC-16

mm, it is very difficult to accurately determine rutting depth in the wheel-tracking test. Thus, the test is not reliable for 0.01 mm precision. For example, in one case the relative deformation is 0.09 mm between 45 min. and 60 min. while in another it is 0.08 mm, whereas the dynamic stability values range from 7000 cycles/mm to 7875 cycles/mm.

(2) Relative deformation ratio

The relative deformation ratio is defined as the deformation due wheel-tracking divided by the sample thickness. Although dynamic stability and relative deformation ratio both represent deformation after loading, the dynamic stability value is a measure of deformation between 45 and 60 min., and does not include deformation prior to the 45 min. point. That is, the intercept of the rutting test curve is not considered in dynamic stability.

On the contrary, the relative deformation ratio can account for the entire deformation process during the test. **Figure 53** shows the relative deformation ratio for different asphalt mixtures; it can be summarized as follows. The relative deformation of A- and B-gradings of asphalt mixtures peaks as the asphalt content is reduced. At the optimum asphalt content, B asphalt mixtures exhibit superior stability at high temperatures as compared with A asphalt mixtures, and there is a large difference between asphalt mixtures. That is, the relative deformation ratio is sensitive to the mixture and to the test variables (asphalt content, grading, and temperature). The low and high asphalt contents selected for this study exhibit significantly different mixture performance at high temperatures.

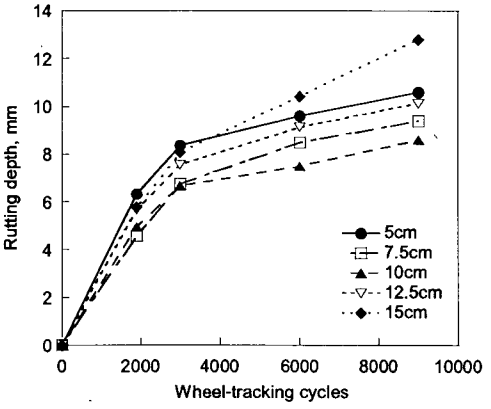

a) AC-13

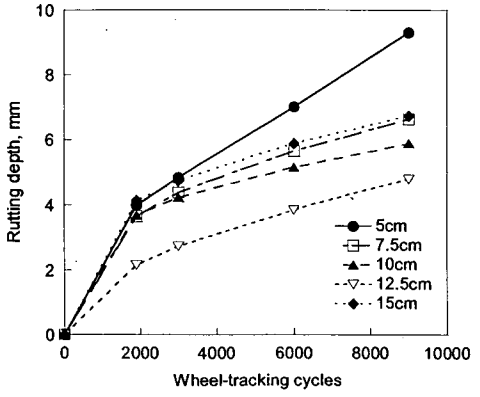

b) AC-20

Figure 55 Relationship between rutting depth and wheel-tracking cycles

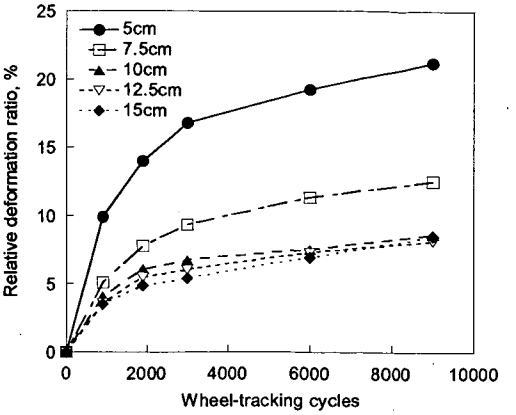

a) AC-13

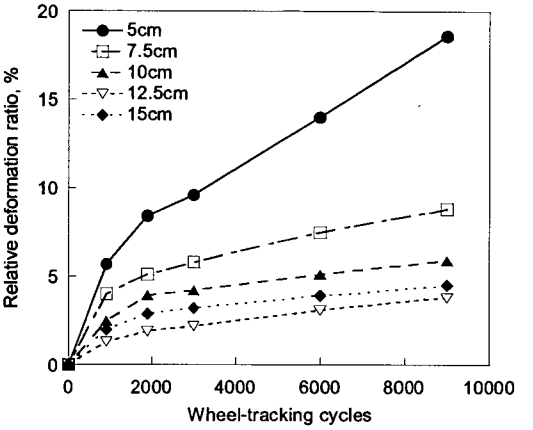

b) AC-20

Figure 56 Relationship between relative deformation ratio and wheel-tracking cycles

(3) Influence of sample thickness on rutting test

In order to evaluate the relative deformation ratio, rutting test results for asphalt mixture samples of different thicknesses are shown in **Figures 55** and **56** and **Tables 41** and **42**.

It can be seen that dynamic stability differs less with varying sample thickness as compared with relative deformation ratio, which varies considerably. However, when the sample thickness is between 10 cm and 15 cm, the relative deformation ratio varies only slightly at different wheel-tracking cycles. That is, for sample thicknesses between 10 cm and 15 cm, sample thickness has little influence on relative deformation.

Table 43 shows the rutting test results for asphalt mixtures usually used in Japan. These values show that dynamic stability changes slightly when slab thickness is increased, but the relative deformation ratio changes significantly. The results for slab thicknesses between 100 mm and 150 mm are relatively close.

Table 39 shows the data for both thicknesses as well as the ratio of percent rut depth at 3000 cycles for 50 mm slabs to the percent rut depth at 30000 cycles for 100

mm slabs. The ratios vary, indicating that the two methodologies will yield different conclusions concerning the rutting potential of a mixture. A ratio of 1.0 indicates that the two tests yielded the same rut depth at the specified maximum number of cycles. Four out of five surface mixtures gave ratios of less than 1.0. A ratio of less than 1.0 indicates that the test using thick slabs is more severe. The rut depth tended to be greater using the 50 mm slab for a given number of wheel passes. Based on these results, a sample slab thickness of 100 mm is suggested when the total pavement thickness for the mixture to be placed is to be greater than 50 mm, or when the asphalt mixture contains aggregate with maximum sizes up to 25 mm. On the other hand, a 50 mm sample is suggested when the mixture will be placed at a thickness of 50 mm or less.

Table 39 Rutting test results for different asphalt mixtures at 60°C

a) 100 mm thick slab

Item	Cycles	Asphalt type				
		AC-5	AC-10	AC-20	Novophalt modified asphalt	Styrelf modified asphalt
Rutting depth (mm)	300	3.0	3.0	2.6	1.4	1.8
	1000	3.8	4.0	3.2	1.7	2.2
	3000	4.9	5.3	4.1	2.2	3.0
	10000	8.2	9.2	4.9	2.4	3.2
	30000 (Spec.)	15.5	13.8	6.4	2.6	3.7
Dynamic stability (cycles/mm)	-	1818	1538	2222	4000	2500
Slope (percent RD vs. cycles)	-	0.35	0.34	0.19	0.14	0.16

b) 50 mm thick slab

Item	Cycles	Asphalt type				
		AC-5	AC-10	AC-20	Novophalt modified asphalt	Styrelf modified asphalt
Rutting depth (mm)	300	3.6	3.4	3.3	1.7	1.8
	1000	5.4	4.5	4.1	2.1	2.3
	3000 (Spec.)	8.3	6.0	5.1	2.5	2.6
	10000	-	10.1	7.4	3.5	3.2
	30000	-	-	11.2	4.4	4.0
Dynamic stability (cycles/mm)	-	689	1333	2000	5000	6667
Percent rutting depth after 3000 cycles (%)	-	16.6	12.0	10.2	5	5.2

c) Ratio of rut depth

	Asphalt type				
	AC-5	AC-10	AC-20	Novophalt modified asphalt	Styrelf modified asphalt
Ratio of rut depth*	0.5	0.4	0.8	1.0	0.7

*Ratio of percent rut depth at 3000 cycles with 50 mm slab to the percent rut depth at 30000 cycles using 100 mm slabs

Table 40 Influence of deformation measurement on dynamic stability

Deformation (mm)	Dynamic stability (cycles/mm)
0.06-0.1	10500-6300
0.11-0.2	5727-3150
0.21-0.63	3000-1000
0.64-0.99	630-63

Table 41 Rutting test results for different sample thicknesses with the AC-13 grading

Thickness (cm)	Rut depth after 9000 cycles (mm)	Dynamic stability (cycles/mm)	Relative deformation ratio at different wheel-tracking cycles (%)		
			3000 cycles	6000 cycles	9000 cycles
5	10.61	797	16.8	19.2	21.2
7.5	9.40	1000	9.3	11.3	12.5
10	8.64	1864	6.7	7.5	8.6
12.5	10.14	1642	6.0	7.3	8.1
15.0	12.7	1692	5.4	6.9	8.5

Table 42 Rutting test results for different sample thicknesses with the AC-20 grading

Thickness (cm)	Rut depth after 9000 cycles (mm)	Dynamic stability (cycles/mm)	Relative deformation ratio at different wheel-tracking cycles (%)		
			3000 cycles	6000 cycles	9000 cycles
5	9.30	1719	9.6	14.0	18.6
7.5	6.63	2115	5.8	7.5	8.8
10	5.88	3333	4.2	5.2	5.9
12.5	4.79	5789	2.2	3.1	3.8
15.0	6.73	2821	3.2	3.9	4.5

Table 43 Rutting test results for different asphalt mixtures

Mixture type	Slab thickness (mm)	Rutting depth (mm)	Dynamic stability, (cycles/mm)	Relative deformation ratio (%)
Dense grading (AC-13)	50	7.01	521	14.0
	100	7.11	538	7.1
	150	8.57	474	5.7
Dense grading (AC-20)	50	6.01	716	12.0
	100	7.11	670	7.1
	150	6.75	583	4.5

(4) Validation of different evaluation indicators

The available evaluation indicators include rutting depth after loading cycles, percent rutting depth, and dynamic stability. In order to determine which of these is most suitable for predicting rutting performance in the laboratory, two sets of data were chosen for validation.

a) Validation of rutting performance for SAC-16 asphalt mixture

In 2000, three test sections with different surface asphalt mixtures were laid on the Shi-huang national freeway in China: SAC-16, SAC-16+Cobel fiber, and SAC-16+Boni polymer fiber. Pavement sections from K32+190 to K33+010 were selected for the field studies, as shown in **Figure 57**. A single pavement cross section for all test sections ensured that any differences in pavement performance were functions of the surface mixture type. Each section consisted of a 4 cm surface mixture, 5 cm AC-20 asphalt concrete course, a 6 cm AC-25 asphalt concrete course, a 20 cm cement-stabilized crushed stone base course, and a 34 cm lime fly ash-stabilized soil subbase course. After one year, rut depth was measured; the results are shown in **Table 44**.

This table shows that the asphalt mixture containing Boni polymer fibers has better resistance to rutting than other asphalt mixtures, and that Cobel fibers did not improve rutting resistance at all. This may be because Cobel is a kind of wood fiber; when added to the mixture, it absorbs some asphalt and so is difficult to compact. The relative deformation ratio as compared to the rutting susceptibility of asphalt mixtures in the laboratory has a direct relation to rutting depth in the field.

b) Validation of rutting performance of difference asphalt mixtures

The performance of ALF (Accelerated Loading Facility) pavement was used to validate a variety of asphalt mixtures for use in rutting prediction **Table 45** and **Table 46** show actual ALF measured depths and rankings based on PRT and ALF pavement performance.

These tables show that the percent rut depth as obtained with the PRT correctly ranked the five surface mixtures based on average data. However, in the relationship between percent rutting and cycles obtained from the PRT test, the following measurement indicators did not rank correctly with ALF: intercept, dynamic stability, and slope.

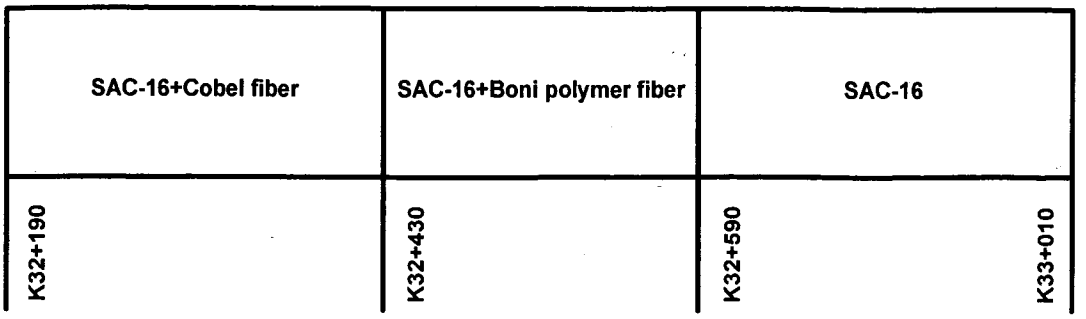

Figure 57 Layout of test sections for in-service test

Table 44 Rutting depth measurement results for test sections of Shi-huang national freeway

Mixture type	Section number	Average rut depth (mm)	Dynamic stability (cycles/mm)	Relative deformation ratio (%)	Ranking based on pavement rutting depth in situ*
SAC-16+Cobel fiber	K32+190-K32+410	4.89	985	16.7	C
SAC-16+Boni polymer fiber	K32+430-K32+570	2.70	984	12.9	A
SAC-16	K32+590-K33+010	4.11	984	14.4	B

*The letter is the statistical ranking, with "A" denoting the mixture with the lowest susceptibility to rutting.

Table 45 Rutting performance based on ALF

Rut depth in asphalt layer (mm)	Number of ALF wheel passes				
	AC-5	AC-10	AC-20	Styrelf	Novophalt
10	130	340	234	7910	293000
15	340	940	984	55540	1750000
20	670	1900	2730	220000	6000000

Table 46 Statistical ranking for the five surface mixtures as obtained with ALF and PRT

Ranking based on pavement rut depth at 58°C	Slope	Intercept	Dynamic stability (cycles/mm)	Relative deformation ratio (%)
Novophalt	0.13	0.7	4000	2.6
Styrelf	0.15	0.8	2500	3.7
AC-20	0.20	0.8	2222	6.4
AC-10	0.37	0.3	1538	13.8
AC-5	0.45	0.2	1818	15.5

6.5 Summary

The following conclusions can be drawn from this analysis:

1) The proposed relative deformation ratio can be used to evaluate the rutting stability of asphalt mixtures at high temperatures. In the laboratory, the **accuracy of** deformation measurements can be used to derive the relative deformation ratio, which is sensitive to different asphalt mixtures and test conditions.
2) Since dynamic stability does not reflect the overall deformation state of the asphalt mixture in rutting tests, and is also affected by the precision of deformation measurements, dynamic stability is not a suitable index for evaluating the rutting susceptibility of asphalt mixtures.
3) A sample slab thickness of 100 mm is suggested when the total pavement thickness for the mixture to be placed will be greater than 50 mm, or when the asphalt mixture contains aggregate with maximum sizes up to 25 mm; on the other hand a

sample slab thickness of 50 mm is suitable for a mixture that will be placed to a thickness of 50 mm or less.

4) Through validation of asphalt mixtures in the field, laboratory values of relative deformation ratio were shown to closely agree with actual rut depths measured in situ.

7. FINAL CONCLUSIONS

Stability and durability are desirable qualities of asphalt mixtures, and are essential to ensuring that structural requirements are met throughout the life of the pavement. However, a number of factors including asphalt type, aggregate grading, additives, and compaction method can affect the stability and durability of asphalt mixtures. A durable, stable mixture requires high-quality asphalt, a dense aggregate grading, and proper air void content. The damaging effects of moisture may be mitigated through the use of hydrated lime or a liquid anti-stripping agent. A sufficient amount of modified binder is also required for a stable and durable mixture to ensure resistance to abrasion under traffic loading. The aggregate grading in the mixture must further be considered in the assessment of durability and stability.

To allow measurement of asphalt mixture performance, it is very important to have available some simple and verified test methods.

ACKNOWLEDGMENTS

The authors would like to express their sincere appreciation to JSPS and NILIM for their support of this study.

(Received Feb. 16, 2004)

REFERENCES

1) Kennedy, T.W.: Prevention of water damage in asphalt mixtures, ASTM, Special Technical Publication (STP), No.899, pp. 119-113, 1984.
2) Kennedy, T.W. and Ping, W.V.: Comparison study of moisture damage test methods for evaluating anti-stripping treatments in asphalt mixtures, Transportation Research Record (TRR), No. 1323, pp. 94-111, 1991.
3) Selim, A.A.: Liquid anti-stripping agents can be advantageous over hydrated lime in resisting moisture-induced damage in asphalt mixtures, Fifth International Conference on the Bearing Capacity of Roads and Airfields, pp. 1173-1182, 1998.
4) *The test specifications of asphalt and asphalt mixtures*, People Communication Press, 2000 (in Chinese).
5) Walsh, G., Mahony, M.O., and Jamieson, I.L.: Net adsorption test for chip-sealing aggregate and binders, TRR, No. 1507, pp. 1-12, 1995.
6) Abdulshafi, O. A., Fitch, M. G., Kedzierski, B., and Powers, D. B.: Laboratory Optimization of Asphalt Concrete
7) Intermediate Course Mixes To Improve Flexible Pavement Performance, Transportation Research Record (TRR), No. 1681, pp. 69-75, 1999.
8) Goodrich, J. L.: Asphalt and Polymer Modified Asphalt Properties Related to the Performance of Asphalt Concrete Mixes, Association of Asphalt Pavement Technologists, Vol.57, pp.116-175, 1988.
9) Izzo, R. P., Button, J. W., and Tahmoressi, M.: Comparison of Coarse Matrix High Binder and Dense-Graded Hot-Mix Asphalt, TRR, No. 1590, pp. 108-117, 1997.
10) Federal Aviation Administration: Measurement, construction, and Maintenance of Skid Resistant Airport Pavement Surfaces, 150/5320-12C, 1997.
11) Civil Aviation Bureau, Ministry of Land, Infrastructure and Transport, Japan: Design Standards on Airport Civil Engineering facilities, 2001 (in Japanese).
12) Sato, K., Fukute, T., Sato, M.: Studies on the Stability of Asphalt Pavement Grooves: Technical Note of Port and Harbor Research Institute, No.308, 24p., 1978.
13) Nomura, K., Maruyama, T., and Takahashi, M.: Study on accelerated aging of asphalt', Journal of Pavement Engineering, Japan Society of Civil Engineers, No.1, pp.223-230, 1996 (in Japanese).
14) Japan Road Association: Handbook for Asphalt Pavement Test Methods, 1069p., 1989 (in Japanese).
15) Jung, D. and Vinson, T.S.: Low Temperature Cracking Resistance of Asphalt Concrete Mixture, AAPT, Vol62, pp.54-92.
16) Jung, D.H. and Vinson, T.S.: Low Temperature Cracking, Test Selection, SHRP-A-400, 1994.
17) Bhurke, A.S. Shin, E.E., and Drzal, L.T.: Fracture Morphology and Fracture Toughness Measurement of Polymer-modified Asphalt Concrete, TRB, No. 1590, pp.23-33, 1997.
18) Zaman, A.A. Fricke, A.L., and Beatty, C.L.: Rheological Properties of Rubber Modified Asphalt, Journal of Transportation Engineering, ASCE, Vol.121, No.6, pp.461-467, 1995.
19) Collins, R., Watson, D., and Campbell, B.: Development and Use of Georgia Loaded Wheel Tester, *Transportation Research Record*, 1995, No. 1492, pp. 202-207.
20) Collins, R., Shami, H., and Lai, J.S.: Use of Georgia Loaded Wheel Tester to Evaluate Rutting of Asphalt Samples Prepared by Superpave Gyratory

21) Zhang, D.: *Asphalt Pavement*, Communication Press of P.R. China, 1998.
22) Carpenter, S.H.: Permanent Deformation: Field Evaluation, *Transportation Research Record*, 1993, No. 1417, pp. 135-143.
23) Jackson, N.M. and Baldwin, C.D.: Assessing the Relative Rutting Susceptibility of HMA in the Laboratory with the Asphalt Pavement Analyzer, *International Journal of Pavement Engineering*, 1999, Vol. 1, pp. 203-217.
24) Stuart, K.D., Mogawer, W.S., and Romro, P.: *Validation of Asphalt Binder and Mixture Tests That Measure Rutting Susceptibility*, 2000, FHWA-RD-99-204.